JOURNAL OF GEOPHYSICAL RESEARCH, VOL. 96, NO. D12, PAGES 22,423–22,445, DECEMBER 20, 1991

Three-Dimensional Simulation of ^{7}Be in a Global Climate Model

RICHARD A. BROST

Max Planck Institute for Chemistry, Mainz, Germany

JOHANN FEICHTER

Meteorological Institute, University of Hamburg, Hamburg, Germany

MARTIN HEIMANN

Max Planck Institute for Meteorology, Hamburg, Germany

In the upper troposphere and lower stratosphere, cosmic rays create Beryllium 7 atoms, which subsequently attach to submicron dust particles, so that wet deposition ultimately removes most ^{7}Be from the troposphere. Because this source is well known and because there is a large climatological data set for ^{7}Be concentration in surface air and deposition on the surface, simulating ^{7}Be provides a good test of the wet scavenging parameterization in a global climate simulation model, such as ECHAM2, which is the European Center for Medium Range Weather Forecasting (ECMWF) model with new physics introduced by the University of Hamburg. A simple parameterization in which the simulated condensation rate determines the scavenging frequency in each grid cell is used in the tracer transport model GLOMAC1, which is embedded in the meteorological model ECHAM2. In this paper we compare observed and model-calculated values of monthly average and annual average surface concentration at a global network of 79 stations. The average absolute value of the error in simulated surface concentration is 1.4 mBq m^{-3} compared with an average observed concentration of 3.5 mBq m^{-3}. At most stations and in most regions the simulated surface concentration has about the correct magnitude and seasonal cycle, although there is a bias so that the modeled concentration is high at mountain stations in the tropics and low at sea level in polar regions. There are less climatological deposition data than there are climatological concentration data, but the model basically simulates the correct latitudinal variation of the zonally averaged deposition, which has a peak at the polar front (30°–50°N), although the model also has a peak produced by convective precipitation in the intertropical convergence zone, a peak that is not observed. We think that ^{7}Be, used in conjunction with other species such as ^{210}Pb, provides an excellent test of wet scavenging in a global model.

1. INTRODUCTION

Mankind is having a growing impact on the chemistry of the atmosphere and thereby on global climate. Numerical models are an important tool to understand and to predict these changes as well as to evaluate the potential effect of various control strategies and emission scenarios, so that it is important to develop global climate models in which chemistry, aerosols, radiation, and clouds interact with one another and with the atmospheric dynamics. The main uncertainty in such atmospheric dynamical models is the parameterization of subgrid-scale processes such as clouds: vertical transport, radiative effects, and wet scavenging, with the last one being the main topic here.

1.1. *Aerosol-Borne Radioactive Tracers*

There is a wealth of atmospheric data on radioactive species that reside on atmospheric aerosols and provide a potentially useful test of scavenging parameterizations. The gas ^{222}Rn is emitted by continental land surfaces and decays with a half-life $\tau_{1/2}$ = 3.8 days through a series of short-lived species (sum of their half-lives of the order of 1 hour) to ^{210}Pb, which has a half-life of 22 years. *Feichter et al.* [this issue] discussed simulation of ^{210}Pb and to a lesser extent ^{222}Rn with the global model also used here. In this paper we focused on ^{7}Be, which has a half-life of 53 days and is created in the upper troposphere and lower stratosphere by spallation reactions, disintegrations of nuclei of nitrogen and oxygen atoms that have been hit by cosmic ray neutrons.

Both ^{210}Pb and ^{7}Be quickly attach to submicron particles, although the radioactive species are in such microscopic amounts that they do not affect the physical and chemical properties of the aerosols, which are generally removed from the troposphere by precipitation. To a first approximation then, the particles carrying ^{7}Be move downward from the upper troposphere until wet scavenged, and those particles carrying ^{210}Pb travel upward from the lower troposphere until wet scavenged. This particular combination of species makes a demanding test of a wet scavenging parameterization, because more data must be matched and because the species should have different transport histories and might enter clouds at different heights. More than 30 years ago, Machta used observed vertical profiles of these two species to test mixing and wet scavenging in a one-dimensional eddy diffusivity model [*Junge*, 1963].

1.2. *Climatological ^{7}Be Data*

To study the meteorological climate produced by a global weather model, for example, researchers typically simulate a period of 20 years and then for variables of interest calculate the average of all Januaries in the 20 years and the standard

Paper number 91JD02283.
0148-0227/91/91JD-02283$05.00

deviation of individual Januaries about the 20-year-average January and, similarly, for other months. Then averages and standard deviations can be compared for the simulated and observed meteorology. A similar procedure should be used to verify modeled and observed chemical climatologies. Of course, such lengthy periods of observations are normally not available for many chemical species of interest, for example, to greenhouse warming, so that it is useful and even necessary to test and to verify a climatological meteorological model on species such as radionuclides, which often have such records available, before applying the model to species that might be of more current environmental interest but probably have less suitable data bases.

To test the climatological model used here, we need climatological data, which implies annual averages and, preferably, monthly averages for as many years as possible in order to have an idea of the interannual variability in the data. Because ^{7}Be needs to be measured in situ, climatological data here mean surface-based data: surface concentration in air and surface deposition, either total deposition or that in precipitation. Concentration data taken aloft in the troposphere and stratosphere can only represent relatively short periods of time and cannot qualify as climatological. Thus we will compare here with climatological, surface-based data.

An important issue is what determines the observed monthly average surface concentration of ^{7}Be. *Feely et al.* [1988] stated that the surface concentration of ^{7}Be depends on four processes: (1) wet scavenging (WS), (2) stratosphere-to-troposphere exchange (STE), (3) downward transfer (DT) in the troposphere, and (4) horizontal transfer (HT) from middle and subtropical latitudes to higher and lower latitudes. In the past, different researchers have emphasized different processes, particularly WS and STE, as controlling the annual cycle of the surface concentration of ^{7}Be at particular stations. For example, *Aegerter et al.* [1966] emphasized that the ^{7}Be in air at the surface should be basically of tropospheric origin, so that the observed annual cycle at the surface should result from the annual cycles in processes other than STE, particularly WS and DT. WS was considered dominant by *Arnold and Al-Salih* [1955], *Cruikshank et al.* [1956], and *Marenco and Fontan* [1974]; however, STE was emphasized by *Parker* [1962], *Schumann and Stoeppler* [1963], *Rangarajan and Gopalakrishnan* [1970], *Reiter et al.* [1971, 1975, 1983], *Reiter and Munzert* [1983], *Viezee and Singh* [1980], and *Dutkiewicz and Husain* [1985]. It seems best to adopt the viewpoint of *Feely et al.* [1988] that at different stations and during different seasons, different processes can determine surface concentration, so that any or all of the four processes might be important.

Each of these four processes has its own seasonal cycle, so that the seasonal cycle of surface concentration of ^{7}Be is some complicated product of the four processes; at different locations, different processes may be dominant, and the seasonal cycle in ^{7}Be can have one or more maxima and a maximum in any season or maxima in many combinations of seasons. For example, STE has a peak in spring and summer near the polar front and subtropical jet streams, so that the annual cycle in ^{7}Be may be dominated by this process at certain middle-latitude stations, especially at high elevations. Similarly, the troposphere is less stable in summer than in winter, so that there is more downward transfer in the troposphere produced by compensating subsidence around convection in summer than in winter; hence certain middle-latitude, continental stations might have concentration maxima in summer produced by this process (as long as the continental, summertime maximum in precipitation does not suppress this concentration maximum). Arctic stations have late winter and early spring maxima owing to the horizontal transport patterns in winter and perhaps also to the lack of wet scavenging in winter. Subtropical stations are dominated by wet scavenging, so that local precipitation and concentration are strongly negatively correlated [*Feely et al.*, 1988]. We take the attitude that the largest uncertainty in our modeling is the wet scavenging, and we are allowed to tune the parameterization until it is no longer true that most of the discrepancy between modeled and observed concentration and deposition is produced by errors in the scavenging parameterization.

There is a long history for observations of ^{7}Be in the atmosphere and in precipitation: *Arnold and Al-Salih* [1955] reported the first observations of ^{7}Be in rainwater, and *Cruikshank et al.* [1956] reported the first observations of ^{7}Be in air. By the middle 1960s, ^{7}Be became relatively easy to measure reliably and has been routinely observed since then by networks and individual field programs.

Networks to monitor radioactive fallout (such as ^{137}Cs, ^{144}Ce, ^{95}Zr, ^{210}Po, ^{90}Sr) have often provided observations of naturally occurring species such as ^{7}Be and ^{210}Pb as (perhaps unintended) side benefits. Concern about fallout caused countries such as the United States and England to set up worldwide networks during the 1950s and 1960s to sample radioactive fallout. (These networks are currently managed by the Environmental Measurements Laboratory, hereafter EML, in the United States and Harwell Laboratory in the United Kingdom. Lead (^{210}Pb) may be artificially produced in atomic blasts [*Turekian et al.*, 1977], but ^{7}Be probably is not [*Lal et al.*, 1960].) After the ban on atmospheric testing in 1963 agreed to by the United States and the USSR, the amount of atmospheric testing decreased, so that the atmospheric concentrations of radioactive debris and interest in monitoring such debris both faded. Following the last open air test, by China in 1980, concentrations of fallout species, such as ^{137}Cs, decayed to unmeasurable levels in the middle 1980s [*Feely et al.*, 1988; *Larsen and Sanderson*, 1990]. The Chernobyl accident in 1986, however, increased interest in maintaining national and global networks to be ready to monitor the next nuclear accident or the next atomic bomb explosion in the atmosphere. Thus additional national networks have been set up in the last few years, and the networks in existence often routinely measure ^{7}Be, sometimes just to stay in practice for observing the more interesting radioactive fallout species.

1.3. *Wet Scavenging*

Wet scavenging is a complex phenomenon that depends on a wide spectrum of spatial scales from the microphysical to the storm scale and beyond; such details are described elsewhere, such as by *Pruppacher and Klett* [1978] and *Hales* [1986]. Because the variables available from a global model are typically averaged over hundreds of kilometers, global modelers have generally not been able to parameterize unambiguously such detailed subgrid-scale behavior. Practical parameterizations that have been used in global-scale models have not used microphysical detail and in

general have descended from the work of *Junge and Gustafson* [1957], who described the wet scavenging of the species whose mixing ratio in cloud is c_{cl}.

$$\frac{\partial c_{cl}}{\partial t} = -\frac{\varepsilon \dot{Q}_{cl}}{L} c_{cl} = -\lambda c_{cl} \quad (1)$$

where ε is the efficiency or fraction of the aerosols that are scavenged, $\dot{Q}_{cl}$ is the rate of production of precipitation in kg m^{-3} s^{-1}, and L is the cloud liquid water content in kilograms per cubic meter. Thus the scavenging frequency $\lambda = \varepsilon \dot{Q}_{cl}/L$. *Junge* [1963] argued that ε is perhaps inversely proportional to the particle density: $\varepsilon = 0.9$–1.0 for maritime precipitating clouds, $\varepsilon = 0.5$–0.8 for continental precipitating clouds and may become as small as 0.2 in the polluted continental planetary boundary layer, but for particles with $r > 0.1$ μm, *Junge* [1977] thought that $\varepsilon = 0.95$–1.0. For typical $L = 1$–3 g m^{-3} [*Mason*, 1957], Junge used (1) and could approximately explain the observed aerosol lifetime and the observed increase of lifetime with height. Junge noted that the main sink of aerosols with radii $0.1 < r < 1.0$ μm is nucleation scavenging, so that to a first approximation such aerosols are either activated and serve as condensation nuclei soon after entering the cloud or they pass through the cloud without being scavenged. (Also, of course, aerosols pass through nonprecipitating clouds about 10 times before encountering a precipitating cloud and then running the risk of being removed from the atmosphere [*Junge*, 1963].) Machta argued that because the production of precipitation decreases with height and the aerosols are activated near the height where they enter the cloud, λ should decrease with height [*Junge*, 1963].

Scavenging parameterizations that have been used in global-scale models generally remove aerosols at the same rate that the meteorological model converts either water vapor or cloud water into rainwater [e.g., *Joussaume*, 1990; *Giorgi and Chameides*, 1986]. Such parameterizations have not gotten much more sophisticated than (1) and mainly differ in the choices either for λ or for ε, L, and $\dot{Q}_{cl}$, particularly how these parameters vary horizontally, vertically, and temporally. For example, work at the Geophysical Fluid Dynamics Laboratory (GFDL) in the United States [*Mahlman and Moxim*, 1978; *Levy et al.*, 1980; *Levy and Moxim*, 1987, 1989] has specified the vertical variation of λ (a decrease with height) but allowed the model-predicted surface precipitation to determine the temporal and horizontal variation of λ. Also, λ was varied depending on the height of the source and the solubility of the aerosol or the solubility and reactivity of the gaseous constituent. *Giorgi and Chameides* [1986] developed a parameterization for the scavenging of very soluble species in which the vertical, horizontal, and temporal variations of λ were chosen by the $\dot{Q}$ predicted in each grid cell of the parent meteorological model. (Note that $\dot{Q} = F\dot{Q}_{cl}$, with F the average precipitating cloud cover.) This parameterization is used here with a somewhat reduced λ for small $\dot{Q}$ because the ^{7}Be is not always borne on very soluble aerosols. *Penner et al.* [1991] used (1) with λ also dependent on the solubility and reactivity of the species being scavenged. Often precipitating clouds do not fill entire grid cells in a global model, and the rate at which the aerosol is depleted from the entire grid cell can be limited by the rate at which the aerosol is supplied from the nonprecipitating part of the grid cell to the precipitating part of the grid cell. Thus λ may depend on the details of the subgrid-scale mixing as well as the details of the scavenging. There is work under way to incorporate much more microphysical and subgrid-scale mixing detail in such global models, and parameterization of subgrid-scale mixing and scavenging will continue to be active areas of research for many years to come.

2. BERYLLIUM 7 SOURCE, BUDGET, AND DISTRIBUTION

2.1. ^{7}*Be Source*

Beryllium 7 is produced naturally in the atmosphere by a cosmogenic source. Primary cosmic rays (mainly protons) tend to travel along the Earth's magnetic field and enter the atmosphere predominantly over the magnetic poles. These protons strike atoms in the upper atmosphere and create a cascade of secondary and tertiary particles, but of interest to ^{7}Be production is the resulting flux of neutrons, which can continue downward in the atmosphere and collide with oxygen and nitrogen atoms to produce nuclear disintegrations, known as "stars," a small fraction of which produce ^{7}Be atoms. The energy of the initial cosmic ray particle determines how deep into the atmosphere the subsequent cascade can penetrate before the secondary and tertiary particles are slowed by collisions and can no longer produce stars. The combination of the rapid decrease with penetration depth of the flux of low energy neutrons and the increase with depth of atmospheric density (that is, the concentration of target nuclei) makes a peak ^{7}Be production in the middle of the atmosphere [*Junge*, 1963]. About 67% of the ^{7}Be source is in stratosphere and the rest is in troposphere [*Lal*, 1963]. A newly produced ^{7}Be atom diffuses until it encounters a particle, to which the atom becomes attached. Because most of the particulate surface area is found on particles with diameters between 0.03 and 1.0 μm, the ^{7}Be atoms usually attach to these submicron particles, and the future of the ^{7}Be atoms becomes that of submicron atmospheric dust. Particles in this range do not grow in size or settle appreciably for height $z < 20$ km but instead just travel with the ambient airflow, so that the ^{7}Be travels with the particle until the ^{7}Be decays radioactively (half-life $\tau_{1/2} = 53$ days) or until the particle leaves the troposphere, normally by being deposited on the surface.

2.1.1. *Magnitude and spatial variation of source.* Not only does ^{7}Be have a large amount of reliable climatological data, appropriate for the testing of a climatological model, but it also has a source that is relatively well known in terms of its total magnitude and its spatial and temporal distributions, as least on the time and space scales of interest to the simulation of ^{7}Be. The source was originally characterized by *Cruikshank et al.* [1956], although the standard description for the ^{7}Be source as a function of altitude and geomagnetic latitude was by Lal and coworkers [e.g., *Lal and Peters*, 1962, 1967; *Lal*, 1963; *Bhandari et al.*, 1966]. More recently, *O'Brien* [1979] used a theoretical yield of ^{7}Be atoms from stars instead of the experimental yield used by Lal and calculated a 33% smaller source; however, we used the original, larger Lal source, as digitized from a plot by *Bhandari et al.* [1966], a discretization that produced an average global source within a few percent of that given by *Lal* [1963]. Nonetheless, the reader should bear in mind that we used the larger source estimate. Also, our source is constant in time, an assumption that is discussed later.

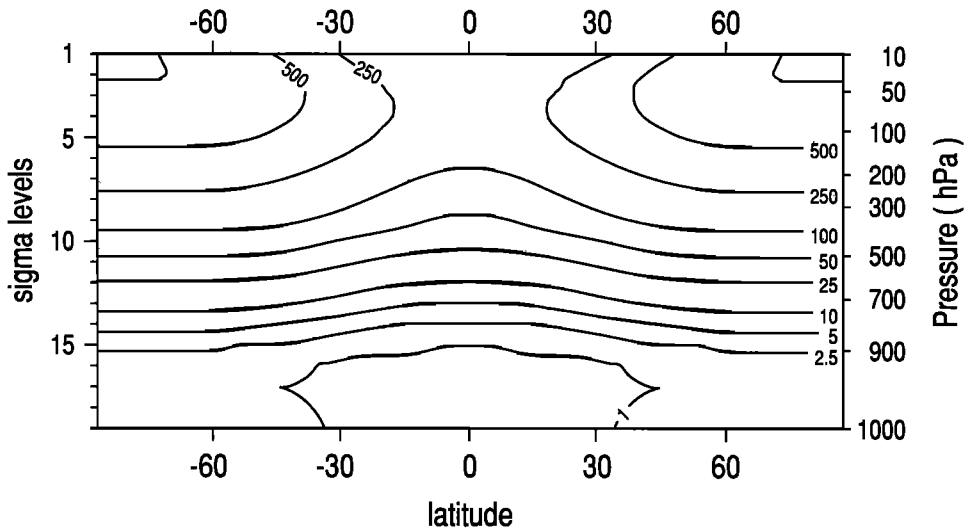

Fig. 1. The beryllium source expressed as the zonal average secular equilibrium concentration of ^{7}Be in mBq m^{-3} (STP).

Furthermore, it would have been better to set up a lookup table for the source in terms of pressure [see *Lal and Peters*, 1967] rather than in terms of height [*Bhandari et al.*, 1966]. Our procedure created a slight, unwanted annual cycle in the extratropical source in each hemisphere, with the simulated January source low and the July source high in the northern hemisphere and a reversed cycle in the southern hemisphere. We estimated that this unwanted annual modulation affected the surface concentration by about ±10% or less. (The zonal average secular equilibrium concentration of ^{7}Be shown in Figure 1 is the concentration, $\bar{c}_{sr}$, that would exist if the cosmogenic source equaled the radioactive decay rate everywhere, and no other processes such as advection, diffusion, or deposition existed. Thus $\bar{c}_{sr}$ is directly proportional to the source. All concentrations of ^{7}Be will be given in millibequerels per cubic meter at STP, or mBq m^{-3}. The concentration in mBq m^{-3} is approximately 1/27 of that in fCi m^{-3}, or 10^{-15} curies per cubic meter.) We used a standard coordinate rotation to convert latitude and longitude to geomagnetic latitude, using a geomagnetic pole near Thule, Greenland [*Matsushita and Campbell*, 1967, p. 1329], although the distinction between magnetic, geomagnetic, and ordinary latitude as well as the movement of the geomagnetic pole with time are probably not important for our results. At each time step in the model we converted from ordinary latitude and longitude to geomagnetic latitude, and also we used the height of the center of each grid box to calculate the source in each box as a function of time. The resulting global source was only approximately constant in time.

We calculated the time τ_{sr} that the zonally averaged source would require to produce the zonally averaged model concentration $\bar{c}$ (ignoring all processes except production and radioactive loss). In the stratosphere at high latitudes, $\tau_{sr} \approx 77$ days, the exponential decay time of ^{7}Be, with a large part of the stratosphere having $\tau_{sr} = 50$–100 days. In the upper tropical troposphere, τ_{sr} can fall below 25 days, because transport decreases $\bar{c}$ below $\bar{c}_{sr}$, that is, transport carries ^{7}Be from this region. Conversely, for $z < 4$ km and latitudes equatorward of 40°–60°, τ_{sr} is often greater than 250 days and ranges above 1000 days, so that in situ production is unimportant there, and ^{7}Be must be imported. This suggests that in this region the effects of transport and scavenging approximately balance, so that this region should provide a simple and hence good test of the two processes. On the other hand, near the surface in the polar regions, τ_{sr} can fall below 100 days, which suggests that the concentration there might result from a delicate balance of as many as four processes (transport, wet scavenging, in situ production, and dry deposition), a balance which might make this a harder region to model well; and we do in fact have trouble in this shallow polar region.

2.1.2. *Cosmic radiation.* Primary cosmic radiation has both a galactic and a solar source and is basically charged particles, about 90% protons and 10% alpha particles with trace amounts of nuclei with atomic numbers up to about 82 [*Friedlander*, 1989]. The majority of the energetic particles have a galactic source, but in traveling across galactic space, the particles have been scattered and quasi-randomized by the weak magnetic fields there, so that the galactic particles approach the solar system isotropically. Similarly, weak and fluctuating magnetic fields in the solar system scatter the solar particles, and the Earth's magnetic field bends the particles around the Earth, so that there is practically no east-west variation in the solar and cosmic particle fluxes into the atmosphere [*Friedlander*, 1989]. Only very energetic charged particles, however, can cross the field lines of the Earth's magnetic field and penetrate into the atmosphere at the equator, but moving toward the geomagnetic poles, particles with lower and lower energy can penetrate into the atmosphere, making a pronounced north-south gradient in the flux of less energetic particles into the atmosphere [*Hillas*, 1972, p. 19]. Galactic protons should dominate the production of ^{7}Be in the atmosphere at all latitudes except for the upper atmosphere in the immediate vicinity of the magnetic poles, where solar protons can be important, but the contribution of solar protons to the integrated production of ^{7}Be in the atmosphere must be a few percent or less [*Lal and Peters*, 1967].

2.1.3. *Temporal modulation of the source.* The ^{7}Be

TABLE 1. Temporal Variability of Surface Neutron Flux

Station	Latitude	z, m	Period	σ*	Minimum	Maximum
Alert, Canada†	+82	57.	1965–1988	5.1/5.3	−8.8/−14.1	+6.2/+8.5
Kiel, Germany	+54	40.	1965–1989	5/NA	−11/NA	+8/NA
Jungfraujoch, Switzerland	+47	3570.	1968–1990	6.8/8.4	−14/−20	+7.7/+18
Huancayo, Peru	−12	3000.	1953–1989	2.2/2.3	−4.5/−7	+3.6/6.0
Dumont D'Urville	−66	35.	1981–1990	6.3/7.9	−9.3/−18	+9.7/+19

*The last three columns show percent deviations. The number before the slash is the deviation based on yearly averaged data and that after the slash is based on monthly averaged data. Thus at Alert the standard deviation of the yearly averaged data is 5.1% of the long-term mean, the minimum yearly average is 8.8% below the mean, and the maximum yearly average is 6.2% above the mean."NA" is not available.

†Data from Kiel based on *Hoetzl et al.* [1991]. All other data were obtained from the National Geophysical Data Center, Boulder, Colorado.

source in the atmosphere undergoes regular and irregular temporal changes on a wide variety of temporal and spatial scales [*Lal and Peters*, 1967]. Some of the discrepancies shown later between observation and model simulation may be explained by the variation in source produced by the 11-year sunspot cycle in particular. Such temporal changes are largely controlled by the Sun through two effects.

The first process is the more or less steady but also variable solar wind, a plasma of relatively low energy particles, that can because of its magnetic fields somewhat inhibit the passage of the galactic cosmic radiation through the solar system to the Earth, so that an "active Sun" (a period with a high sunspot number) actually decreases the galactic cosmic radiation received at the Earth and thus reduces the ^{7}Be source. (The temporal behavior of the neutron flux in the atmosphere should indicate the temporal behavior of the ^{7}Be source. At zero temporal lag the neutron flux at the surface at Kiel has a correlation coefficient $r < -0.8$ with the average sunspot number [*Hoetzl et al.*, 1991].) Since the very energetic galactic particles are less affected by the solar wind and the (more affected but) less energetic particles from the Sun are generally unable to cross the Earth's magnetic field at low geomagnetic latitudes, the temporal changes in cosmic radiation increase with geomagnetic latitude. In addition, such temporal changes also increase with height in the atmosphere, because the lower the energy of the primary particle the less the particle and its descendants can penetrate into the atmosphere before collisions sap their energies [*Lal and Peters*, 1967; *Friedlander*, 1989].

Because of the sunspot cycle the ^{7}Be source had a local maximum in 1954 and a local minimum in 1958. For these extreme years, *Lal and Peters* [1967] calculated that averaged from 1000–300 hPa the variation in the annual average tropospheric source was ±4% equatorward of 45° and ±12% poleward of 45°. Above the troposphere this modulation did not change with height at the equator, but at 80° geomagnetic latitude the variation increased with height to ±50% at 50 hPa. More recent data generally agree with the conclusions of *Lal and Peters* [1967].

Table 1 summarizes the temporal variations we found in long-term records of neutron flux at the surface of the Earth. The standard deviation of annual average neutron flux (σ_{yr}) is about 2% of the long-term mean in the tropics and about 5–7% in middle and high latitudes. Because the largest amplitude fluctuation in the source near the surface is produced by the 11-year sunspot cycle, the standard deviation of monthly average neutron flux hardly exceeds σ_{yr}. Although ^{7}Be is generally imported to the tropics from middle latitudes and the stratosphere, and thus concentrations at tropical stations might be affected by the temporal changes in the source in middle latitudes or the stratosphere, it is very difficult to find an 11-year modulation of concentration at a tropical station. Thus when we deal with data averaged over months or longer, the error produced by ignoring temporal changes in the source should always be much less than 10% in the tropics. During extreme months, however, the source at the surface in high latitudes and at high elevations in middle and high latitudes can differ by as much as 20% from the long-term mean (Table 1).

We found little if any annual cycle in the neutron fluxes at the stations in Table 1: the amplitudes were relatively small (less than or much less than 2% of the mean, when the fluxes were corrected to constant pressure). Note that the neutron flux depends on the mass of atmosphere above the point, that is, the pressure, but at a constant height in the extratropical middle troposphere there is an annual cycle in neutron flux just because there is an annual cycle in the mass of air above the point: in summer the air heats and expands so that pressure surfaces rise, the air mass increases above a fixed height in the middle troposphere, and hence the neutron flux at the fixed height decreases. Thus there was a ±5% annual cycle at the Jungfraujoch, but when the flux was corrected to constant pressure, this cycle disappeared, indicating the general lack of an annual cycle in the cosmic ray flux at the top of the atmosphere and in the ^{7}Be source.

Irregular variations in the ejection of particles by the Sun, the second solar modulation process, can increase or decrease the ^{7}Be source for hours or days. On time scales less than 1 month, neutron monitors at the surface see the following effects: 27-day cycles corresponding to the Sun's rotation rate as seen from the Earth; Forbush decreases, of a few to 20%, which can last for a few days; diurnal variations of 0.1–0.2% (our analyses of the data in Table 1 gave a suspiciously large 2% at Huancayo and tenths of a percent or less at other stations); and occasional sudden increases produced by solar flares [*Hillas*, 1972; *Friedlander*, 1989]. These amplitudes may increase with height, particularly in polar regions. Because of solar flares, perhaps less than once per year the neutron flux at the surface increases by an order of magnitude, but this increase rapidly decays with a half-life of 1–2 hours [*Hillas*, 1972, p. 123); 10 times per year there can be flare-produced increases that last days and dominate the proton flux in the top of the atmo-

sphere near the magnetic poles [*Lal and Peters*, 1967]. However, because we compare the data averaged for at least 1 month and because $\tau_{1/2}$ = 53 days, these short-term fluctuations in source strength should not change the concentration more than a few percent.

2.1.4. *Annual average neutron flux and surface ^{7}Be concentration.* In addition, we did some further analysis to search for evidence of the sunspot cycle in the records of annual average concentration. We found 24 stations that had at least 10 years of concentration data, and for each station we correlated the observed annual average surface concentration with the observed annual average neutron flux at Kiel. At eight stations $r < 0$ and at 16 stations $r > 0$: correlations ranged from −0.5 to 0.93 and averaged 0.26, which is not significantly different from zero at the 95% confidence level, based on an average sample size of 17 years per station. Of the 24 stations, seven had statistically significant positive correlations and one had a statistically significant negative correlation at the 95% confidence level. There was a slight tendency for significant positive correlations to occur at middle and high latitudes of the northern hemisphere.

As a measure of the magnitude in the interannual variability in observed surface concentration we took the 24 stations with long-term records, divided each annual average concentration by the station's long-term average, and then averaged the resulting signals to produce a relative concentration factor for each year. This concentration factor varied more than the neutron flux at Kiel: the standard deviation between yearly values of the factor was 9% and the extreme excursions were −18% and +17% of the long-term mean. The annual average concentration factor had a correlation coefficient of only 0.27 with the annual average neutron flux at Kiel, so that year-to-year fluctuations in annual average concentration exceeded interannual changes in source strength, and the normally small amplitude variation in source strength produced by the sunspot cycle cannot easily emerge above the fluctuations in annual average surface concentration produced by meteorological variability, for average data records of 17 years. Clearly, stations can be found with statistically significant positive correlations between annual average concentration and annual average surface neutron flux (and these stations tend to be in the northern hemisphere at high latitudes and high elevations), but often the variability in meteorology, on scales from days to years, obscures this relationship.

2.1.5. *The ^{7}Be source: conclusions and possible improvements.* Of course, the temporal modulation of the source is only important in middle and particularly in high latitudes. The error in annual average concentration or deposition can probably be greater than 10%, but only in polar regions for stations with short data records that were taken near extrema of the sunspot cycle, during particularly large flare events or Forbush decreases or during large transport events from the upper troposphere and the stratosphere. In general, however, we believe that averaging over multiple years of data rapidly tends to remove the effects on concentration produced by the sunspot cycle modulation of the source. Errors in the source term of these magnitudes probably affect the simulated deposition and concentration less than the uncertainties in scavenging do. Finally, because the O'Brien and Lal estimates of the total source strength differ by 33%, using a temporally constant source seemed a justifiable first step.

TABLE 2. Simulated Annual Average ^{7}Be Budget for the Atmosphere

Process	^{7}Be, g/month
Source	11.55
Radioactive decay	6.82
Total deposition	4.73
dry deposition	0.30 (6.3%)*
wet deposition	
stratiform	2.58 (54.5%)
convective	1.85 (39.1%)

*Percentage of total deposition.

In the future, taking a more rigorous account of the effect of the temporal modulation by the Sun of the ^{7}Be source would be possible but perhaps not easy. The simplest action would be to use the neutron flux to identify periods with large flares, Forbush decreases, or extrema of the sunspot cycle, and exclude short records of ^{7}Be data taken at polar stations during such periods. Trying to scale either the model data or the concentration data based on the variation with time of the source during the sunspot cycle could be ambiguous because of the variation with latitude and height of the amplitude of the sunspot-induced source change. Perhaps three model runs, one with the polar tropospheric source, one with the polar stratospheric source, and the final one with the equatorial source could be used to find the contribution to the concentration and deposition at any point and then to scale the contributions based on the year in the sunspot cycle. We could go much farther and actually simulate the cycle. Following *Lal and Peters* [1967] it would be straightforward to calculate a source that varied yearly based on the variation in the cycle, but this has several disadvantages. First, we would need an 11-year simulation. Second, our data base would have less statistical significance for any single year: even the best station would only have 1 or 2 years of data for each year in the generic solar cycle. Third, the cycle is not uniform because of the presence of longer time scales. These approaches do not seem worth the effort now.

2.2. *^{7}Be Budget*

Table 2 gives the model-simulated budget of ^{7}Be for the whole atmosphere, which is dominated by the stratosphere. The ^{7}Be loss is 59% to radioactive decay and 41% to deposition, largely wet deposition, particularly wet deposition in stratiform precipitation. For the troposphere only, an approximate budget would show a source of 3.8 g/month produced locally in the troposphere, with an additional 1 g/month entering from the stratosphere. The sink would be 4.4 g/month lost to wet deposition and 0.3 g/month lost to dry deposition, with a trivial loss to radioactive decay. These model results generally agree with analyses of the data [e.g., *Lal*, 1963]. Therefore to a first approximation, ^{7}Be produced in the stratosphere decays radioactively without ever leaving the stratosphere, and ^{7}Be produced in the troposphere is wet scavenged before it has a chance to decay radioactively. Because the primary loss process for ^{7}Be in the troposphere is wet scavenging, modeling ^{7}Be should provide a good test of wet scavenging.

2.3. *Use of ^{7}Be to Study Transport*

Some researchers used ratios of the concentrations of ^{7}Be and other radioactive species with similar source distributions but different $\tau_{1/2}$s to estimate the lifetimes of air parcels, particularly the average time before the parcel is cleansed by precipitation scavenging [*Raisbeck et al.*, 1981; *Shapiro and Forbes-Resha*, 1976], although *Rangarajan and Eapen* [1990] criticized this use of ^{7}Be.

Many investigators have used ^{7}Be as tracer of transport, particularly of the stratospheric circulation [*Bhandari*, 1970*a*; *Reiter et al.*, 1975] and of the stratospheric contribution to ^{7}Be in tropospheric air [*Young et al.*, 1970; *Rangarajan and Gopalakrishnan*, 1970; *Reiter et al.*, 1971; *Dutkiewicz*, 1985; *Dutkiewicz and Husain*, 1979, 1985; *Reiter et al.*, 1983; *Reiter and Munzert*, 1983]. For example, ^{7}Be has often been correlated with O_3, with both having high concentrations indicating stratospheric air [*Reiter et al.*, 1983]. *Wolff et al.* [1979] found peaks of surface O_3 and ^{7}Be on the backside of surface high pressure systems. *Dutkiewicz and Husain* [1985] estimated that on an annual and global average, 25% of ^{7}Be observed at the surface came from the stratosphere, with 40% coming from the stratosphere in spring and summer. Of course, individual locations could have even larger percentages of stratospheric contribution.

Rangarajan and Gopalakrishnan [1970] and *Feely et al.* [1988] correlated the seasonal cycles of ^{137}Cs and ^{7}Be to estimate the percentage of ^{7}Be that came from the stratosphere. A nuclear explosion is the only important atmospheric source of ^{137}Cs. Except for the first few months after the explosion, ^{137}Cs in the troposphere must have come from the stratosphere and is thus a direct measure of STE. Of course, to the extent that processes other than STE are responsible for the seasonal cycle of ^{7}Be, and if the seasonal cycle of ^{7}Be is coincidentally in phase with that of ^{137}Cs, then this analysis falsely attributes a stratospheric source to ^{7}Be. *Feely et al.* [1988] determined that during spring and fall about all of the surface ^{7}Be at Point Barrow, Alaska, and Kap Tobin, Greenland, came from the stratosphere. For Thule, Greenland, and many stations in middle latitude and high latitude North America, they inferred that the stratosphere contributes 30–50% during spring and 5–25% during fall.

Viezee and Singh [1980] extensively analyzed EML ^{7}Be data to determine spatial and temporal patterns of surface concentration, particularly the percentage of surface concentration that came from the stratosphere. They concluded that in the annual mean a larger percentage of the surface ^{7}Be came from the stratosphere in the northern hemisphere than in the southern hemisphere and that the maximum percentages were found in northern hemisphere spring, with April having 40% or more. Surface ^{7}Be was found to have a strong positive correlation with the number of surface low pressure troughs in the same latitudinal belt. Analyses of ^{7}Be seasonal cycles indicated that STE had a maximum in summer for 40°–50°N (that is, over North America) and in late winter and early spring for 20–30°N [*Viezee and Singh*, 1980], although extending this analysis procedure to 20°–30°N seems potentially misleading because of the importance of WS in determining the observed annual cycle of ^{7}Be surface concentration there [*Feely et al.*, 1988].

In summary, ^{7}Be has been a popular tool for studying STE, and the inferred seasonal and interhemispheric patterns of STE are consistent with other analyses of STE, but the sensitivity of the annual cycle of ^{7}Be to processes other than STE, as well as the fact that only 25% of the ^{7}Be at the surface comes from the stratosphere, suggests that ^{7}Be may not always be a good species for studying STE. Probably middle-latitude, high-elevation stations are most likely to have the seasonal cycle of ^{7}Be dominated by STE, but it seems misleading to consider the seasonal cycle in ^{7}Be concentration to be exclusively produced by the seasonal cycle in STE for stations near sea level in polar and tropical latitudes.

As an aside we note that we made some preliminary perpetual January and perpetual July runs with ECHAM2/GLOMAC1 (described later) in which we kept separate track of the tracer concentration resulting from the tropospheric source of ^{7}Be and from the stratospheric source of ^{7}Be. For these 2 months it was easy to determine that zonally averaged, the smallest stratospheric contribution to surface concentration occurred in the Arctic in January (10%) and the largest contribution was at about 30°N in July (25%). Because of storage requirements we did not continue to keep separate track of the two parts of ^{7}Be when we began runs with full annual cycles, runs that are the basis of this paper. Thus we cannot do an easy analysis of the stratospheric contribution to surface concentration as a function of latitude and season; for example, we do not know how large the simulated contribution would get in northern hemisphere spring. Nonetheless, the maximum simulated 25% contribution in July is consistent with many data analyses cited earlier and implies that the model does not simulate too much stratosphere-to-troposphere flux of ^{7}Be (assuming that the model-simulated λ is not excessive). But the minimum 10% contribution in January is small compared to some data analyses, and we later show that the model often underpredicts the surface concentration in the Arctic in January. This suggests that a stratospheric contribution may be missing there, but we do not believe the suggestion. Even though the model apparently has problems with transport to the Arctic in January and perhaps with wet scavenging, transport all the way from the stratosphere would not be required to explain the observed concentrations at sea level in the Arctic in January. This is discussed more later.

2.4. *^{7}Be Deposition Data*

Figure 2 shows the location of deposition observations used here. In general, there are less deposition data than concentration data: there are fewer stations, and fewer stations have more than a single year of data. Because the lack of multiple years of deposition data reduces the climatological significance of the data and because precipitation in nature and in the model is so variable from point to point and time to time, we have just compared annual average deposition from the model and from the data.

2.4.1. *Over the ocean.* Measurements of ^{7}Be inventory in the oceanic mixed layer can yield the total (dry and wet) deposition. From the GEOSECS campaign, *Young and Silker* [1980] presented ^{7}Be deposition data for the Pacific Ocean from 30°S to 60°N and from the Atlantic Ocean from 10°N to 55°N. They found an average sink of 0.027 atoms cm^{-2} s^{-1}, which is just slightly larger than the Lal and Peters worldwide value of 0.022 atoms cm^{-2} s^{-1}. Our model also finds larger deposition averaged over the GEOSECS

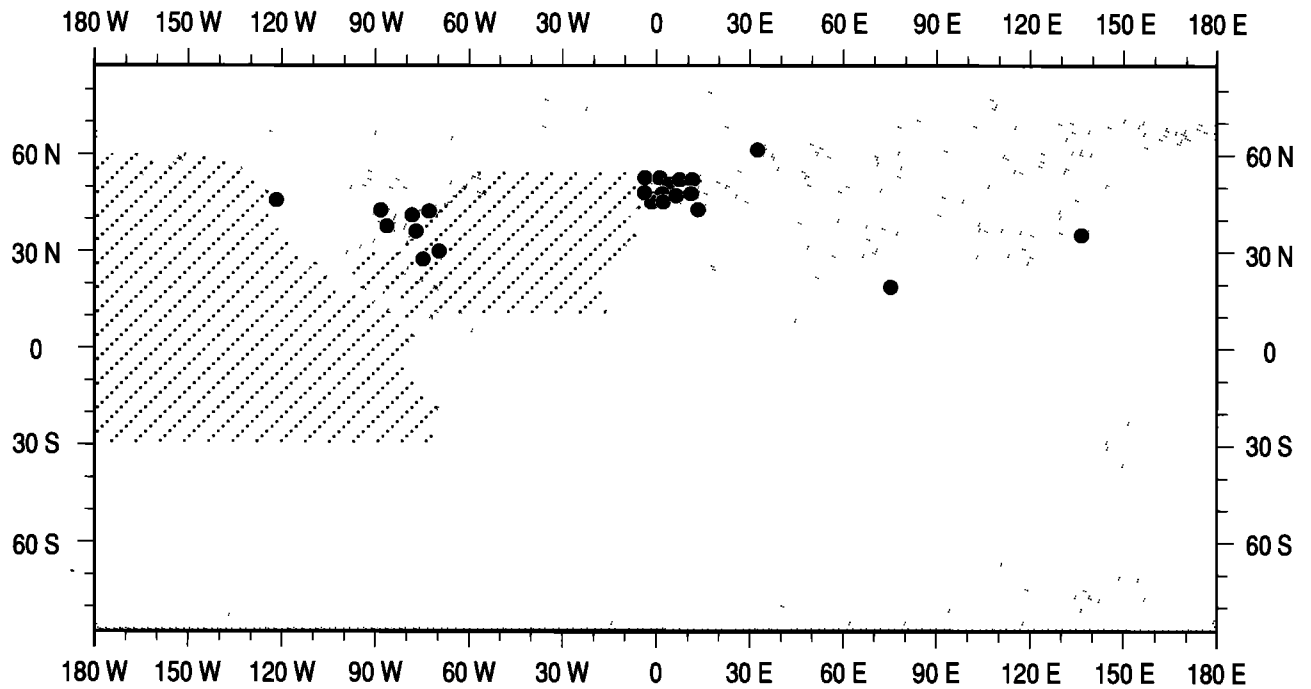

Fig. 2. Locations of deposition data. Dots show 23 land stations with records of one or more years of deposition in precipitation (see text). Cross hatching shows region of GEOSECS data of *Young and Silker* [1980].

ocean region than zonally averaged over the same latitudinal bin (shown later).

Young and Silker [1980] had 30 locations with vertical profiles of ^{7}Be across the top 100 m of the oceanic mixed layer. In most cases the ^{7}Be concentration at a depth of 100 m had decayed to less than 10% of that in the surface water. In a few profiles the surface water of the ocean was overturning, and the concentration at 100 m was hardly reduced from that at the surface. Then they assumed that the concentration tapered to zero between 100 and 200 m depth. From the observed variation of the mixed layer depth with latitude they parameterized the inventory of ^{7}Be in the oceanic mixed layer (and hence the total deposition) in terms of the observed concentration in surface water. They then applied this parameterization to about 200 surface observations to estimate the deposition at each location of a surface observation. These values were averaged into 10° latitudinal bins.

Beryllium 7 has about the ideal lifetime for this data analysis procedure: it lives a few months, during which time it mixes down normally less than 100 m, mixes somewhat horizontally, and can travel horizontally by advection for less than 10° of latitude or longitude. There were many surface observations distributed across the two oceans, but each measurement gives an oceanic concentration averaged over a few months but not over a year. The possibility that some horizontal mixing occurred in the previous few months is good if the mixing extended no more than a few degrees horizontally (a plausible assumption), because this mixing would help to give a more statistically robust, spatially integrated observation. Horizontal advection is not helpful, so if the decay time scale of the species was much longer than that of ^{7}Be, then the species could move too far during a decay lifetime, and all spatial deposition information would be lost. If the lifetime were much shorter than that of ^{7}Be, say, 1 day, then there would have to be far more observations to have any climatological significance. Thus ^{7}Be has about the perfect half-life (long enough but not too long) to make an observation of concentration in surface water a useful temporal average and spatial average measure of deposition and perhaps a better spatial than temporal average because there are 200 data points; although the data are not truly climatological, they are nonetheless interesting and useful.

2.4.2. *Over the land.* Observations of the deposition of ^{7}Be in precipitation yield the wet deposition only, although data [*Brown et al.*, 1989] and model results (Table 2) suggest that wet deposition accounts for more than 90% of the total deposition. (When no dry deposition observations were available, we have used the observed wet deposition as the total deposition; however, in all cases the modeled results represent total deposition.) In general, wet deposition is reported either as deposition or as the concentration in precipitation, which when multiplied by the precipitation gives the deposited amount. *Bleichrodt* [1978] argued that observed concentration in precipitation should be averaged over 10° latitude bins and then multiplied by the zonally averaged precipitation to estimate the zonally averaged wet deposition. In fact, at a single location the concentration in rain depends on the season and on the duration and intensity of the precipitation event. In addition, stations in a region the size of France can consistently differ a factor of 10 in concentration in precipitation, which is greater than the difference in concentration in air moving horizontally across such an area. (Differences in concentration in precipitation might have a physical basis in differences in the height at which air enters clouds.) Since the concentration in precipitation can differ so greatly, we took a simple approach and averaged the annual average deposited amounts into 10° latitude bins for comparison with the model.

We found 23 stations (over land) with one or more years of ^{7}Be wet deposition data. (See Commissariat à l'Energie

Atomique [1987*a*, *b*, 1988*a*, *b*, *c*, *d*, 1989*a*, *b*, 1990*a*, *b*, *c*, *d*], *Bleichrodt* [1978], *Todd and Wong* [1989], *Turekian et al.* [1983], *Crecelius* [1981], and *Dibb* [1989]; sometimes these papers contain data published earlier.) These data constitute a very incomplete picture of the global average wet deposition over land, because the data are largely from the United States and Europe (Figure 2). We did not use data presented by *Harvey and Matthews* [1989] for a west-facing mountain slope in New Zealand because the total rainfall and the concentration of ^{7}Be in rainwater were both so high compared to other sites that the New Zealand data could not be a representative of the zonal average deposition or concentration in precipitation. We also did not use precipitation data from the Jungfraujoch [*Luder*, 1985] because the high elevation made the data unrepresentative.

2.5. *Observed ^{7}Be Atmospheric Concentration*

2.5.1. *Surface concentration.* Let us first review some of the data available and data analyses that have been performed and later specify and describe the data used here. There have been several analyses of the surface concentration data collected by the U.S. network over the Americas. For example, *Viezee and Singh* [1980] noted that the latitudinal pattern features minima in concentration near the equator and poleward of 40°N and 30°S, with some weak suggestions of double peaks in the middle-latitude maxima. Later, *Dutkiewicz* [1985] analyzed the seasonal cycles in different latitude bands; for 10°–30°N and 70°–90°N the peaks were in March to April; and for 30°–70°N the peaks were in June or June and July. If STE basically occurs between 30° and 60° in each hemisphere and afterward the ^{7}Be spreads north and south in the lower troposphere [*Feely et al..*, 1988], then the peaks in polar and subtropical latitudes should lag those in middle latitudes, but the observed peaks lead those in middle latitudes. This suggests that the seasonal cycle of surface concentration cannot result largely from the seasonal cycle in STE, except perhaps in middle latitudes.

There were several early studies that contained data that we did not use because the data did not have monthly averages for at least 1 year. For example, *Bhandari et al.* [1966] had some old data on ^{7}Be, and *Roedel* [1970] gave some ^{7}Be surface concentration data at Heidelberg. *Bleichrodt* [1978] summarized annual average surface data at many stations.

Table 3 summarizes the 79 stations with monthly average surface concentration data used here as well as the more than 50 sources (publications, reports, and private communications), although the majority of the stations were from EML reports by *Feely et al.* [1988] and *Larsen and Sanderson* [1990]. In addition, *Peirson* [1963] gave about 2 years of ^{7}Be in air (and rain) near Chilton, England, but we used instead the 23-year average concentration data supplied by C. Johnson (private communication, 1991) of Harwell. The average number of months of data per station is 90, and the median number of months is 48. In general, we put more trust in the comparisons at stations that have longer data records and more recent data. For example, the concentration at Heidelberg, based on a short record of old data, seems suspiciously low compared to the nearby station at Offenbach, which has a longer record of data from the 1980s.

2.5.2. *Concentration samples above the surface.* As mentioned previously, vertical profiles involve measurements taken over short time periods and not monthly or yearly averages, so they cannot be considered climatological data. *Young et al.* [1970] took observations often enough to try to describe the annual cycle of concentration at eight heights from the surface to 19 km at 46°N, 117°W. At 9–12 km the seasonal cycle had its largest amplitude compared with annual average concentration. The timing of the peak concentration at each height was as follows: z = 0 km, July; z = 6–12 km, June; but z = 12–15 km also had a December to January peak, which was probably produced by the seasonal displacement of the tropopause height; and z = 19 km, again June. The June peak in the upper troposphere may be caused by STE, with the 1 month lag in the peak at the surface perhaps resulting from the time required for the ^{7}Be to propagate downward. *Bleichrodt* [1978] showed ^{7}Be as a function of altitude over the Netherlands and estimated the tropospheric content of ^{7}Be. From commercial 747s, *Dutkiewicz and Husain* [1979] measured O_3 and ^{7}Be at z = 10–12 km and latitudes 21°–55°N. Samples identified based on the O_3 concentration as being taken in stratospheric air had ^{7}Be concentrations within the range given by *Lal and Peters* [1967] for $\bar{c}_{sr}$ at the appropriate latitude and height or as little as 1/2 the lower bound of the range. Tropospheric samples had concentrations from 1/2 to 1/20 of $\bar{c}_{sr}$ because transport and deposition processes reduced the concentrations there. Of course, the percentage of samples that were stratospheric increased moving poleward, as the tropopause generally moves downward. *Drevinsky et al.* [1964] had ^{7}Be concentration at 20 km over United States and noted some evidence for artificial production, that is, the production of ^{7}Be in nuclear explosions, although *Lal et al.* [1960] concluded that nuclear weapons did not result in significant production of ^{7}Be. (The possibility that nuclear explosions produced ^{7}Be was another reason for omitting data before 1970.) Various researchers presented old upper tropospheric and lower stratospheric data, including *Bhandari* [1970*a*, *b*] and *Bhandari et al.* [1966].

3. MODELING SYSTEM AND RUNS

We used the global climate simulation model known as ECHAM2, which is the ECMWF model with some new physics introduced by the Meteorological Institute of the University of Hamburg, version 2 [*Roeckner and Schlese*, 1985; *Roeckner et al.*, 1989*a*, *b*]. The new physics includes radiative transfer [*Rockel et al.*, 1986], explicit moisture (following *Sundquist et al.* [1989]), horizontal diffusion [*Boer et al.*, 1984; *Laursen and Eliasen*, 1988], and soil moisture and surface canopy parameterization [*Duemenil and Schlese*, 1987]. ECHAM2 has been extensively applied and validated in climate studies [*Cess et al.*, 1989; *Barnett et al.*, 1989; *Cubasch et al.*, 1990; *Latif et al.*, 1990; *Windelbrand*, 1990].

The chemical and tracer transport model known as GLOMAC1 is embedded (on-line) in the meteorological model ECHAM2 and is described in more detail by *Feichter et al.* [this issue]. An arbitrary number of tracers can be run on-line with the meteorological model; we used three: ^{222}Rn, ^{210}Pb, and ^{7}Be, although only the last one is discussed here. The parameterization of vertical subgrid-scale transport by clouds followed *Kuo* [1974] and was described by *Feichter et al.* [1991].

TABLE 3. Stations With Surface Concentration Data

Station	Latitude	Longitude	z, m	Observed	Modeled	Months
Nord, Greenland[a]	80.67	−17.00	250.	2.89	1.05	19
Thule, Greenland[a]	76.60	−68.58	259.	3.40	1.65	73
Barrow, Alaska[a]	71.17	−156.50	4.	1.77	1.68	149
Kap Tobin, Greenland[a]	70.42	−21.98	22.	2.70	1.26	80
Vardo, Norway[b]	70.35	31.03	10.	1.48	1.84	14
Tromso, Norway[b]	69.65	18.95	10.	1.81	1.95	117
Skibotn, Norway[b]	69.35	20.33	10.	1.48	1.95	170
DYE-3, Greenland[c]	65.17	−44.73	2560.	2.57	3.11	12
Composite, Sweden[d]	61.00	17.00	100.	2.54	2.33	12[u]
Nurmijarvi, Finland[e]	60.50	24.80	40.	2.22	2.50	24
Riso, Denmark[f]	55.50	12.10	10.	2.55	3.02	266
Bornholm, Denmark[f]	55.00	14.90	10.	2.47	3.19	79
Mace Head, Ireland[g]	53.32	−9.85	25.	2.55	2.90	15
Berlin, Germany[b]	52.60	13.30	50.	2.78	3.47	78
Braunschweig, Germany[b]	52.30	10.60	90.	2.51	3.42	309
Chilton, United Kingdom[h]	51.60	−1.40	30.	1.53	3.14	276
Moosonee, Canada[a]	51.27	−80.50	10.	3.12	3.03	211
Sutton, United Kingdom[i]	51.00	0.00	30.	1.43	3.11	17
Offenbach, Germany[j]	50.15	8.70	130.	2.34	3.55	47
Heidelberg, Germany[k]	49.40	8.70	150.	1.58	3.63	14
Verdun, France[l]	49.20	5.30	90.	2.77	3.54	36
Paris, France[l]	48.80	2.40	90.	3.07	3.48	36[v]
Munich, Germany[j]	48.20	11.60	200.	4.25	3.78	48
Schauinsland, Germany[m]	47.80	8.00	1300.	3.32	4.15	24
Zugspitze, Germany[n]	47.40	11.00	2960.	3.52	5.17	207
Dijon, France[l]	47.30	5.10	110.	3.86	3.75	36
Fribourg, Switzerland[o]	46.80	7.20	585.	3.33	4.08	144
Helena, Montana[a]	46.60	−112.00	1187.	4.39	5.17	59
Beaverton, Oregon[a]	45.53	−122.88	64.	2.48	4.28	119
Bordeaux, France[l]	44.70	−0.70	30.	3.49	3.79	36
Whiteface Mountain, New York[d]	44.00	−74.00	1500.	4.10	4.94	31
Rexburg, Idaho[a]	43.80	−111.83	1502.	5.54	6.30	118
Toulouse, France[p]	43.60	1.50	200.	2.35	4.22	51
Toulon, France[l]	43.10	5.90	20.	5.58	4.36	27
Argonne, Illinois[a]	41.68	−87.97	160.	4.22	4.22	35
New Haven, Connecticut[g]	41.32	−72.92	25.	3.59	3.95	36
Chester, New Jersey[a]	40.80	−74.67	268.	4.25	4.04	146
Salt Lake City, Utah[a]	40.77	−110.82	1516.	7.28	7.13	46
New York, New York[a]	40.73	−74.00	56.	4.58	4.02	221
Rocky Flats, Colorado[a]	40.00	−105.18	1814.	5.64	6.29	121
Sterling, Virginia[a]	38.97	−77.42	76.	4.26	4.32	46
Richmond, California[a]	37.93	−122.33	20.	3.33	5.33	48
Tracy, California[a]	37.65	−121.53	392.	5.16	5.63	48
Gibraltar[d]	36.15	−5.30	20.	3.03	5.57	12[w]
Fullerton, California[q]	33.70	−117.90	30.	8.04	6.85	23
Bermuda[g]	32.30	−64.88	20.	4.88	4.22	28
Izania, Teneriffe[g]	28.43	−16.48	2376.	5.51	8.32	18
Miami, Florida[a]	25.82	−80.28	7.	5.26	4.36	214
Mauna Loa, Hawaii[a]	19.47	−155.60	3401.	7.54	7.15	205
Bombay, India[r]	19.00	73.00	20.	3.32	7.44	13
San Juan, Puerto Rico[a]	18.43	−66.00	10.	4.08	3.95	38
Barbados[g]	13.17	−59.35	50.	3.41	4.52	27
Balboa, Panama[a]	8.97	−79.57	23.	2.40	3.07	65
Merida, Venezuela[a]	8.60	−71.17	1570.	3.58	3.90	22
Pico Espejo, Venezuela[a]	8.58	−71.17	4767.	3.60	7.53	22
La Aguada, Venezuela[a]	8.58	−71.15	3450.	3.90	3.72	21
Guayaquil, Ecuador[a]	−2.17	−79.87	7.	1.86	3.95	210
Lima, Peru[a]	−12.02	−77.13	13.	4.92	5.63	211
American Samoa[a]	−14.25	−170.57	77.	2.63	3.36	145
Chacaltaya, Bolivia[a]	−16.35	−68.12	5220.	5.47	8.65	213
Rarotonga[s]	−21.15	−159.45	8.	2.72	3.90	44
Antofagasta, Chile[a]	−23.62	−70.27	31.	4.13	6.11	198
Easter Island[a]	−27.17	−109.43	41.	2.81	4.55	199
Norfolk Island[a]	−29.00	168.00	10.	4.66	4.22	68
Roleystone, Australia[a]	−32.00	116.00	100.	4.34	4.39	73
Santiago, Chile[a]	−33.47	−70.70	520.	4.94	5.23	196
Kaitaia, New Zealand[s]	−35.12	173.27	86.	3.16	3.73	45
Cape Grim, Australia[a]	−41.00	145.00	10.	3.20	3.31	74
Lower Hutt, New Zealand[a]	−41.20	174.90	10.	2.93	3.39	15
Puerto Montt, Chile[a]	−41.45	−72.95	7.	2.35	3.41	206
Hokitika, New Zealand[s]	−42.72	170.97	40.	2.47	3.27	45
Chatham Island[a]	−44.00	−176.00	100.	3.25	3.04	64

TABLE 3. (continued)

Station	Latitude	Longitude	z, m	Observed	Modeled	Months
Invercargill, New Zealand[a]	−46.43	168.35	10.	2.55	2.88	69
Falkland Islands[a]	−51.82	−58.45	68.	2.18	2.55	18
Punta Arenas, Chile[a]	−53.13	−70.88	35.	1.30	2.48	199
Antarctic Station[a]	−64.82	−62.87	10.	1.48	1.61	31
Dumont D'Urville[t]	−67.00	143.00	10.	6.67	1.27	180
Mawson, Antarctica[a]	−67.60	62.88	10.	6.21	1.69	9
South Pole Station[a]	−90.00	−180.00	2800.	4.24	2.33	193

Table shows station name, latitude, longitude, elevation, observed and modeled annual average ^{7}Be concentration, and months of data.
[a]*Feely et al.* [1988] and *Larsen and Sanderson* [1990].
[b]*Kolb* [1970, 1971, 1974, 1978, 1980, 1984, 1986, 1988, 1990].
[c]J. Dibb (private communication, 1990).
[d]*Dutkiewicz* [1985].
[e]*Paakkola et al.* [1987].
[f]A. Aarkrog (private communication, 1991).
[g]W. Graustein (private communication, 1991).
[h]*Dutkiewicz* [1985] and C. Johnson (private communication, 1991).
[i]*Parker* [1962].
[j]*Toepfer* [1986], and A. Bayer (private communication, 1991).
[k]*Schumann and Stoeppler* [1963].
[l]*Commissariat à l'Energie Atomique* [1987*a*, 1987*b*, 1988*a*, 1988*b*, 1988*c*, 1988*d*, 1989*a*, 1989*b*, 1990*a*, 1990*b*, 1990*c*, 1990*d*].
[m]H. Keller (private communication, 1991).
[n]W. Seiler and R. Sládkovič (private communication, 1991).
[o]*Luder* [1985].
[p]*Marenco and Fontan* [1972].
[q]*Shapiro and Forbes-Resha* [1976].
[r]*Gopalakrishnan et al.* [1973].
[s]*Matthews* [1989, 1990] and K. M. Matthews (private communication, 1991).
[t]*Lambert et al.* [1990].
[u]Composite of several stations and years.
[v]Composite of one–four stations.
[w]May be composite of several years.

As is common in meteorological models, ECHAM2 produces precipitation from two kinds of cloud: convective and stratiform. The partitioning of precipitation and scavenging between the two kinds of cloud will differ from model to model, and in ECHAM2 the global precipitation is divided about equally between convective and stratiform.

The rainout of ^{7}Be is explicitly calculated in terms of the model-generated average condensation rate in a grid cell $\dot{Q}$ following a scheme by *Giorgi and Chameides* [1986, hereafter GC86]. This assumes that all the aerosol in the cloudy air is in the aqueous phase and that the rate of conversion β of liquid water to rainwater is also the rate of removal of aerosol. If we substitute $\dot{Q}_{cl} = \beta L T_c/\Delta t$ in (1), then the change in mixing ratio in cloud produced by a single precipitating cloud of duration T_c that occurred within a model time step Δt would be

$$\Delta c_{cl} = -\varepsilon \beta T_c c_{cl}. \tag{2}$$

If $\dot{Q}_{cl}$ was the result of a very large number of clouds in the same air mass (same part of the grid cell), then the following total change would result [*Junge*, 1963; GC86]

$$\overline{\Delta c_{cl}} = -(1. - e^{-\varepsilon \beta T_c})\overline{c_{cl}}. \tag{3}$$

Because the clouds only occupy a fraction F of the grid cell, the rate of change of the grid cell average concentration $\bar{c}$ would be

$$\frac{\partial \bar{c}}{\partial t} = -\frac{F}{\Delta t}(1. - e^{-\varepsilon \beta T_c})\bar{c}. \tag{4}$$

Note that because the clouds are assumed to keep occurring in the same part of the grid cell, rather than appearing randomly throughout the cell, F appears multiplying the right-hand side of (4) rather than in the exponential.

In (4), GC86 used $\varepsilon = 1$ and parameterized F and β separately for stratiform and convective clouds. For stratiform clouds

$$F = \frac{F_0}{1 + \beta_0 \tau_s}, \tag{5}$$

$$\beta = \frac{\beta_0}{F_0} + \frac{1}{F_0 \tau_s} \tag{6}$$

where a scavenging time parameter for stratiform clouds is $\tau_s = L_s/\dot{Q}$, with the L_s the liquid water content of stratiform clouds. The constants $F_0 = 0.8$ and $\beta_0/F_0 = 10^{-4}$ s^{-1}, following GC86; and $T_c = \Delta t = 40$ min.

For convective clouds, $\beta = 1.5 \times 10^{-3}$ s^{-1} and

$$F = \frac{0.3\Delta t/T_c}{\Delta t/T_c + 0.3\beta\tau_c}. \tag{7}$$

Here the scavenging time for convective clouds $\tau_c = L_c/\dot{Q}$, with L_c the liquid water content of convective clouds and $T_c = 25$ min, a typical duration of the mature stage of a cumulonimbus cloud.

For the liquid water contents within clouds, GC86 used $L_s = 0.5$ kg m^{-3} and $L_c = 2.0$ kg m^{-3}. GC86 regarded their parameterization as providing the scavenging limit for very

TABLE 4. Average Height of Center of Model Level

k	z, km
1	30.94
2	23.67
3	20.41
4	18.10
5	16.08
6	14.13
7	12.24
8	10.43
9	8.71
10	7.10
11	5.62
12	4.30
13	3.14
14	2.17
15	1.39
16	0.793
17	0.386
18	0.146
19	0.032

soluble gases and aerosols, but in GLOMAC1 these parameters led to excessive scavenging in stratiform clouds for small and medium values of $\dot{Q}$ ($<10^{-6}$ kg m^{-3} s^{-1}) and perhaps moderately low scavenging in convective clouds, so that we used $L_s = L_c = 1.5\ 10^{-3}$ kg m^{-3}. Using the original values in ECHAM2 gave surface ^{7}Be concentrations about one half those observed in tropical regions and from 1/10 to 1/100 those observed in polar regions. (The slight change in τ_c for convective clouds from those values used by GC86 did not have a significant global effect, although we note later that increasing τ_c for convective clouds would have provided somewhat better agreement with deposition data near the equator over the ocean.) *Penner et al.* [1991] also chose a scavenging parameterization that gave λ close to that of GC86 for large $\dot{Q}$ but gave a smaller λ than that of GC86 for small $\dot{Q}$. When ECHAM2 was used to simulate the climatic effect of Kuwaiti oil fires [*Bakan et al.*, 1991], τ_s and τ_c were made 3 times larger than the values used here in order to simulate the lower solubility of soot particles than of the particles (often sulfate particles) that carry ^{7}Be. If the global aerosol lifetime is defined as the mass of aerosol in the atmosphere divided by the flux into the atmosphere, then the factor of 3 changes in L_s approximately doubled the global lifetime for soot particles. Although raindrops are allowed to evaporate in ECHAM2, we ignore this in the aerosol budget because an aerosol kernel would not be released unless the drop completely evaporates [*Pruppacher and Klett*, 1978]. For the rather unimportant loss process of dry deposition we used a constant dry deposition velocity of $v_d = 10^{-3}$ m s^{-1}.

We used the original advection scheme from the ECMWF model, which is spectral in the horizontal and finite difference in the vertical. The ^{7}Be concentration field is sufficiently smooth that we encountered no problems representing large horizontal gradients with the spectral advection scheme. The resolution was relatively coarse in the horizontal (5.6° × 5.6°), but the 19 vertical levels (Table 4) provided a rather fine resolution compared to other global tracer and chemistry simulations. For example, *Heimann and Feichter* [1990] compared simulations of ^{222}Rn by three models, GLOMAC1, TM1 [*Heimann and Keeling*, 1989], and MOGUNTIA [*Zimmermann*, 1988; *Zimmermann et al.*, 1989; *Feichter and Crutzen*, 1990], and noted that only GLOMAC1 had sufficient vertical resolution to represent the high surface concentrations of ^{222}Rn found over continents during winter. The meteorological part (ECHAM2) required 5 hours of CPU time on a CRAY2 per year simulated, with each tracer (GLOMAC1) needing only a few percent more.

Related off-line modeling at GFDL [*Mahlman and Moxim*, 1978; *Levy and Moxim*, 1987, 1989] used finer horizontal resolution (about 2.5°) but coarser vertical resolution (only 11 levels) than we used here. H. Levy, II (private communication, 1990) felt that the GFDL experience was that the horizontal resolution was more important than the vertical resolution in determining a realistic simulation of STE and that the fine horizontal resolution used by GFDL was necessary. We found, however, that we did not flood the troposphere with ^{7}Be coming from the stratosphere, so that the resolution used here seemed acceptable for ^{7}Be, but of course on an annual average only 25% of the tropospheric ^{7}Be comes from the stratosphere.

We ran the model (with an annual cycle but without a diurnal cycle) for a period of 4 years and 2 months but only analyzed the final 1-year period. Between the first and second year we made a major change in the scavenging parameterization (*Ls*), and between the second and third years and between the third and fourth years we made minor changes in *Ls*. After making the final change at the start of the fourth year, we let the model adjust for 2 months and then analyzed the subsequent 1-year period. Even with no changes in parameterizations, if we had continued to run the model, each succeeding modeled year would have been slightly different. Further work is needed to see how large this interannual variability in the model-simulated ^{7}Be field would be, although we believe that the uncertainty in surface concentration associated with the interannual variability in meteorology is probably greater than the effect on concentration of the sunspot cycle source modulation.

4. Comparison of Model Simulation With Data

4.1. *Deposition*

Because the concentration of ^{7}Be varies relatively slowly in space at a fixed elevation and because the deposition is a vertical and temporal integral over concentration, the annual average deposition simulated by the model varies smoothly. (In Figure 3 and subsequent plots we show annual average deposition expressed as average deposition per month.) The total deposition naturally reflects the annual precipitation pattern. Minima in deposition, with values less than 5 fg m^{-2} month^{-1} or even less than 2.5 fg m^{-2} month^{-1} (fg is femtogram or 10^{-15} g), can be seen at high latitudes, across the deserts of northern Africa and Saudi Arabia and under the subtropical high pressure systems off the west coasts of the Americas, Africa, and Australia. Maxima above 10 fg m^{-2} month^{-1} can be found at middle latitudes, over the oceans in particular, as well as under the intertropical convergence zone (ITCZ).

The zonally averaged deposition simulated by model usually has three peaks, which move with the Sun and the meteorological seasons. (See the profiles for January and July in Figure 4*a*. The units shown are customarily used for deposition: disintegrations per centimeter squared per month.) The two middle-latitude peaks are produced by

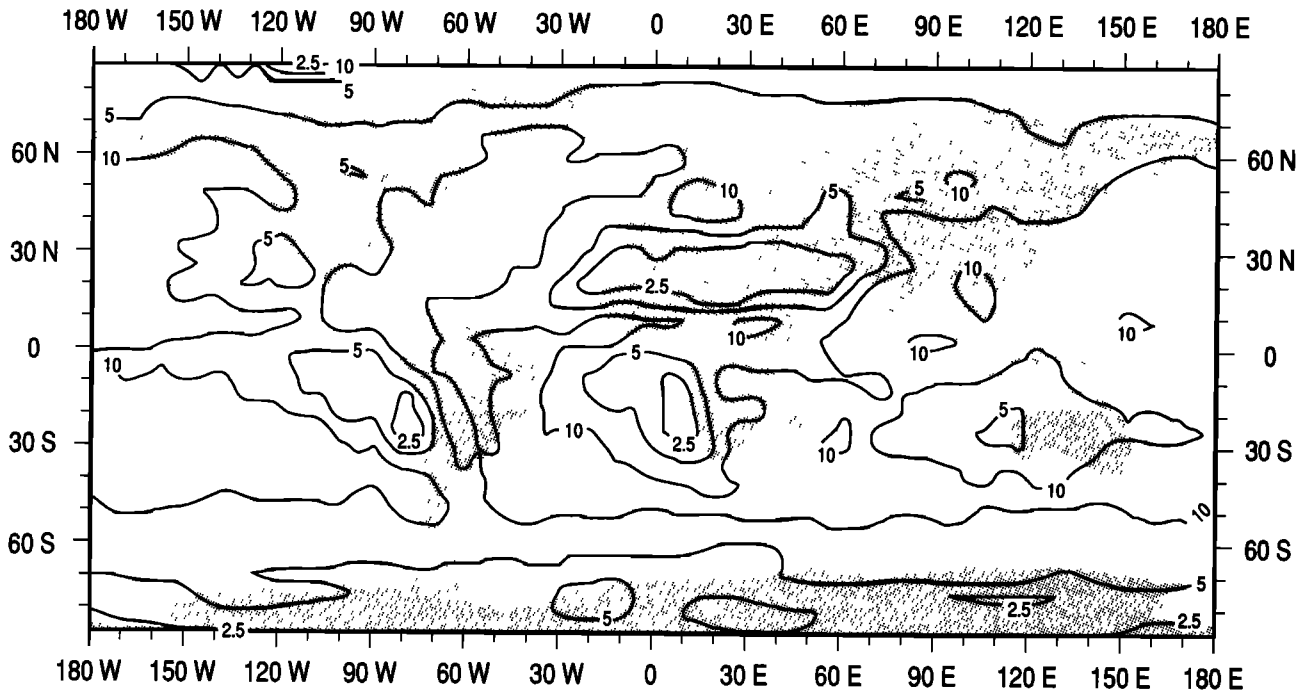

Fig. 3. Annual average total simulated ^{7}Be deposition in fg m^{-2} month^{-1}.

stratiform precipitation in the polar frontal zones, and the equatorial peak is produced by convective precipitation in the ITCZ.

Figure 4*b* compares observed and simulated deposition. Model values were zonally averaged around the globe and shown at the model's latitudinal resolution of 5.6°. Observed values were averages over regions and stations shown in Figure 2. The observed deposition over the land and over the ocean are remarkably similar. In addition, the simulated and observed deposition both have the peak at 30° to 50°N produced by the polar front. The model also simulates a peak at the ITCZ in the region from 0° to 15°N, although the data do not have one and in fact have a minimum between 0° and 10°S. Perhaps here is a weak indication that the model has too much scavenging and wet deposition by convective clouds. But because the GEOSECS data are not climatological data averaged over several years, we did not rerun the model with a new, larger value of L_c. We do note that when we used the original values of L_c and L_s in the GC86 paper, over 80% of the wet deposition was by stratiform clouds, and the zonally averaged plot like Figure 4*b* did not have a deposition peak at the ITCZ. Our increase of L_s and τ_s for stratiform clouds lowered the deposition by stratiform clouds and allowed the ITCZ deposition peak to emerge. Similarly, increasing L_c for convective clouds (or lowering L_s) would remove the ITCZ peak and give somewhat better agreement with the deposition data.

In Figure 4*c* the annual average simulated deposition has been zonally averaged over the GEOSECS region and compared with observations. The general trend in the data is well represented by the model, but modeled values are as much as 30% higher than those observed in the GEOSECS region. Note that the oceanic data have a hint of a peak from 0°–10°N, although the peak is nowhere near as pronounced as in the model. Model deposition is not smoothed horizontally by mixing and advection as in the observations, so that the modeled peaks can be somewhat sharper. Simulated concentration and deposition are linear in the total source strength, so that we would multiply the model concentration and deposition by 0.67 to estimate model values that would be produced by using the *O'Brien* [1979] source. In general, simulations with the two sources would bracket the data, except for the modeled ITCZ peak.

The modeled deposition for 30°–60°N is larger over the ocean than over the land (Figure 4*d*) because the model simulates more precipitation over the ocean than over the land. On the other hand, the simulated surface concentrations are higher over the land than over the sea (not shown) for two reasons: first, higher elevation makes the land surface closer to the source; and second, lower precipitation over the land reduces the loss to wet scavenging. The modeled deposition over the land and over the ocean generally bracket the observations in the northern hemisphere, but again the GEOSECS value for 0° to 10°S, which just applies to the Pacific Ocean, is anomalously low compared with the modeled values. The agreement withthe deposition data is basically quite good, and we decided that the climatologically insignificant deposition data did not justify further tuning of the deposition parameterization.

4.2. *Concentration*

The number of stations with surface observations and the climatological significance of the data records is fairly large compared with that normally available for many species of interest to atmospheric chemistry. The stations are sufficiently numerous and widespread to give a useful picture of the variation in surface concentration with latitude, longitude, and elevation (Figure 5), but the station density is not good enough to analyze to a regular grid and then to compare the observed and modeled values at the grid points; instead we compared at the individual stations.

For each station we found the mean surface concentration for each month of the year and then compared the observed

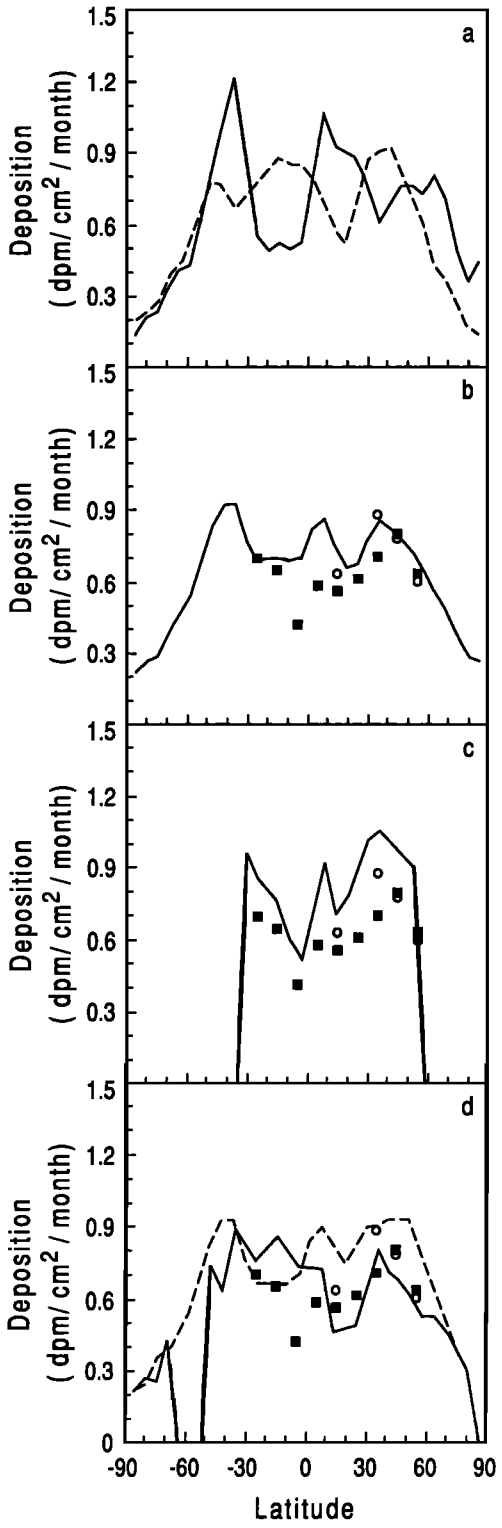

Fig. 4. (*a*) Latitudinal dependence of simulated ^{7}Be deposition in dpm cm^{-2} month^{-1} for January and July. (*b*) Comparison of latitudinal dependence of annual average ^{7}Be deposition for model (zonal average values shown by curve), data taken over the ocean (average for GEOSECS region shown by solid squares), and wet deposition data taken over the land (average of 23 stations shown by open circles). (*c*) Comparison of latitudinal dependence of annual average ^{7}Be deposition for model (average of GEOSECS region shown by curve) and data: solid squares and open circles indicate data as in Figure 4*b*. (*d*) Comparison of latitudinal dependence of annual average ^{7}Be deposition for model and data: solid squares and open circles indicate data as in Figure 4*b*; solid curve is the model average over the land; dashed curve is the model average over the ocean.

monthly and yearly means with the model-simulated values. The high density of stations in Europe and North America means that there are more stations in the northern hemisphere than in the southern hemisphere (56 and 23, respectively). In addition, the asymmetry in land distribution and station placement means that the southern hemisphere has only three stations above 100 m, whereas the northern hemisphere has 14 stations with elevation $z > 500$ m and 24 stations with $z > 100$ m. Thus the average concentration at stations in the northern hemisphere exceeds that in the southern hemisphere because of the importance of elevation in determining concentration. The asymmetric distribution of land and of stations between the hemispheres and the complexity of the seasonal cycles may be the reasons why generally neither the model nor the data show seasonal cycles shifted by 6 months between stations in similar latitude belts of the northern and southern hemispheres.

The annual average surface concentration simulated by the model varies smoothly and is somewhat zonal, particularly at high latitudes (Figure 6). (For the simulated concentration, normally at the surface, we used m for the monthly average and $\bar{m}$ for the annual average. Similarly, o and $\bar{o}$ represent observed monthly and annual averages.) The effect of high surface elevation is obvious in the large $\bar{m} > 10$ mBq m^{-3} over the Tibetan plateau. The subtropical high pressure regions have subsiding currents that bring down high values of ^{7}Be as well as a lack of precipitation and of removal by wet scavenging: the two factors combine to produce relatively high $\bar{m} > 5$ mBq m^{-3} under the subtropical highs. The wet scavenging in the ITCZ also produces the minimum $\bar{m}$ at the equator between the subtropical highs, particularly over the Americas and off the west coast of Africa. The region in the west central Pacific with $\bar{m} < 2.5$ mBq m^{-3} also probably results from this scavenging in the ITCZ. The 2.5 mBq m^{-3} isoline in middle latitudes is almost east-west, and the polar regions have minimum $\bar{m} < 1$ mBq m^{-3}, although we show later that a main failing of this simulation is that near sea level in polar regions, $\bar{m}$ is often low compared with $\bar{o}$.

4.2.1. *Bias, error, and correlation.* The annual cycle of the bias in modeled surface concentration is the average of $o_i - m_i$ over a set or subset of stations, with o_i the observed value and m_i the modeled value at the i^{th} station. For the 79 surface stations the model bias is slightly negative when averaged over the year (Figure 7*a*), and this bias has an annual cycle: the bias is positive in December through February (that is, the model underpredicts) and negative for March through November (model overpredicts), although this average bias (<1 mBq m^{-3}) is small compared to average surface concentrations of 2–8 mBq m^{-3}. Most regions shown in Figure 7*a* also have a similar annual trend in bias. (It is important to note that the annual cycle in the bias was probably not caused by our small but erroneous annual cycle in the source, because the bias has the same phase globally, but our unwanted modulation shifted phase between the hemispheres.) Except for polar stations the bias is always small compared to $\bar{o}$ and o. Stations 30°–60°N have a bias of about −1.3 mBq m^{-3} during northern hemisphere summer, but we later show that this is not large compared to the average concentrations there (4–10 mBq m^{-3}). Again, we note that there is no obvious shift of 6 months in the seasonal cycle of bias between middle-latitude stations in the two hemispheres. Because we have few stations poleward of 60° and because the stations in Antarctica and in the Arctic

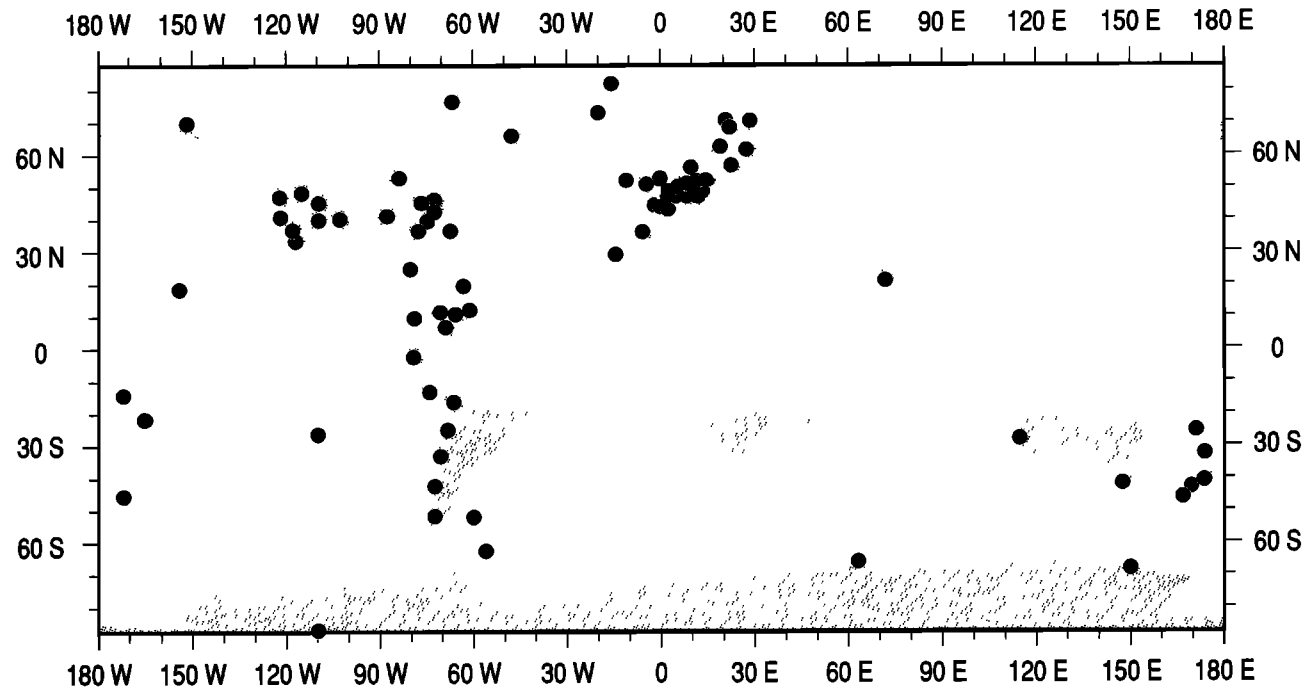

Fig. 5. Locations of 79 stations with observed monthly average surface concentration of ^{7}Be.

sometimes show a similar annual trend (and not a seasonal trend shifted by 6 months between the hemispheres), we have aggregated all polar stations. The most obvious model problem is the large positive bias for polar stations, a bias that in northern hemisphere winter is large compared with o and m there. We will later note that this problem only occurs in the lowest 1 km of a relatively small portion of the surface of the Earth, that is, the polar regions, where we have relatively few stations.

The annual cycle at the 79 stations of the average absolute error e is shown in Figure 7*b*. Globally, e = 1.3–1.5 mBq m^{-3}, with only a small annual cycle. The stations from 30° to 60°S have the smallest e but also have relatively small m. There is again a large annual cycle in e for stations 30°–60°N, but this cycle is in step with the cycle in m, so that annual cycle of e/m is not so large. This measure of model verification and others are consistent in indicating that the simulation is poor in polar regions during December through February.

In order to measure how well the model simulated the observed annual cycle at each station we calculated the correlation coefficient r between observed and simulated monthly average concentration at each of the 79 stations. Because r can be very misleading, such correlations should

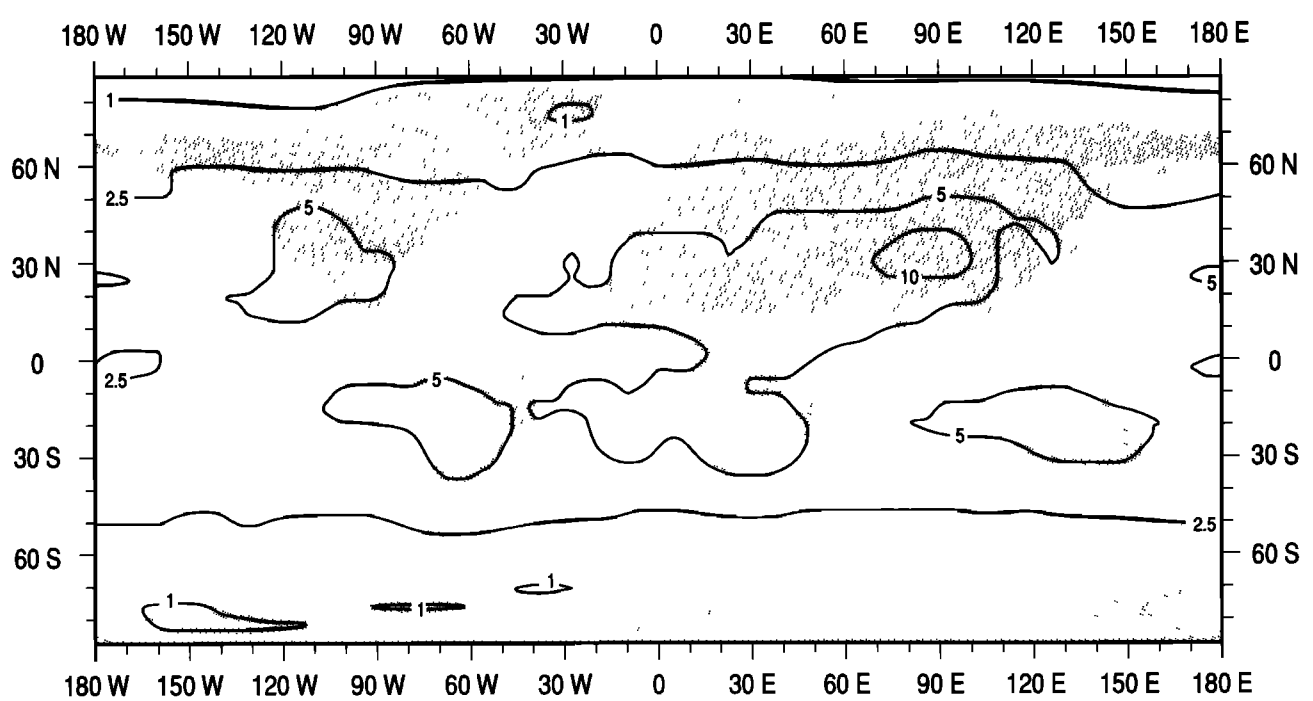

Fig. 6. Annual average ^{7}Be concentration (mBq m^{-3}, STP) in lowest model layer.

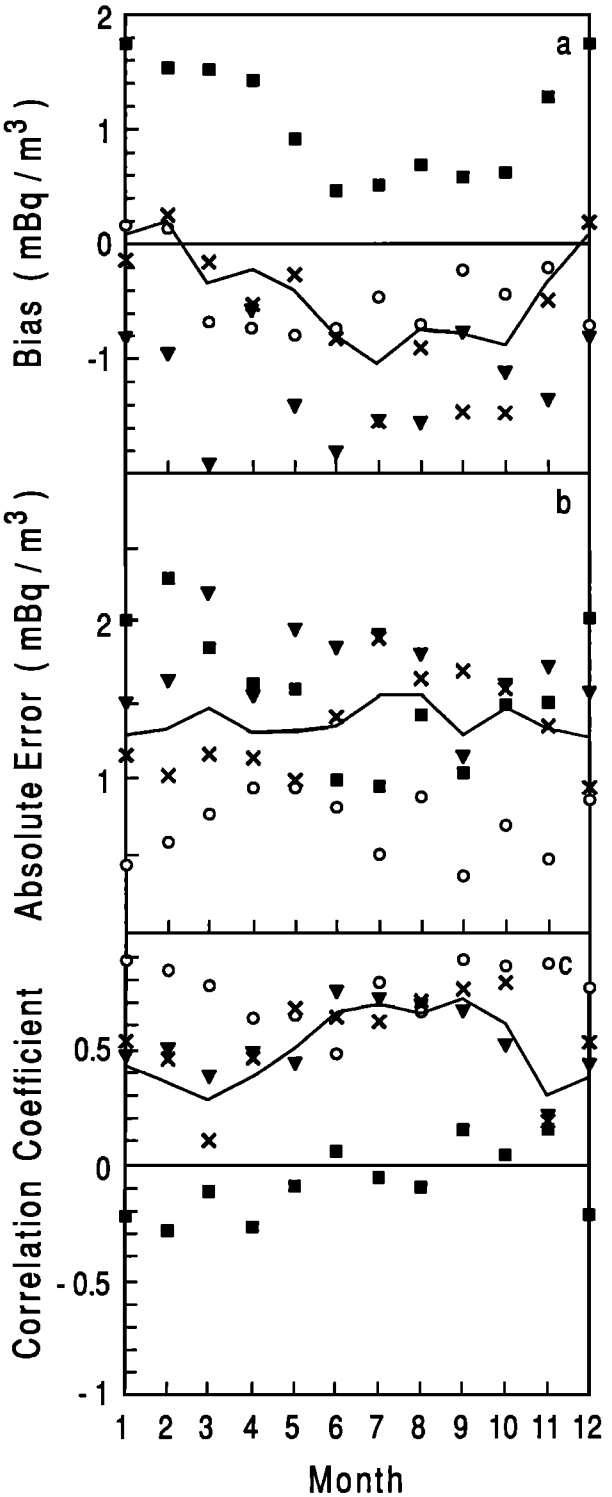

Fig. 7. (*a*) Average model bias (observed minus modeled concentration in mBq m^{-3}) at the 79 stations: solid curve is global average, crosses indicate stations 30°–60°N, open circles indicate stations 30°–60°S, solid triangles indicate tropical stations 30°S–30°N, solid squares are stations poleward of 60°. (*b*) Average absolute values of error in model-stimulated concentrations at stations. (*c*) Correlation coefficient versus month for different regions.

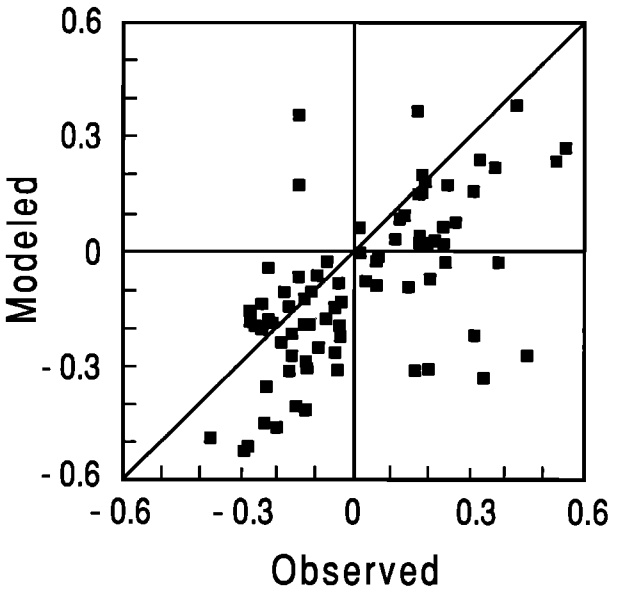

Fig. 8. Modeled versus observed seasonality S = (DJF − JJA)/(DJF + JJA) for 79 stations, with DJF the average concentration in December, January, and February and JJA the average concentration in June, July, and August. Note that southern hemisphere stations were not shifted 6 months relative to northern hemisphere stations.

be considered with several cautions in mind. First, r is useful only if the amplitude of the seasonal cycle is large. Second, even if $r \approx 1$, this tells nothing about whether $\bar{m}$ is close to $\bar{o}$. Third, with only 12 data points (that is, months), r must be greater than 0.57 to be significantly different than zero at the 95% level. Fourth, r is extremely sensitive to results at a few outlying points and thus is not a robust statistic.

Figure 7*c* shows the correlation coefficient r among all the stations for the individual months. Here r measures how well the model reproduces the concentration differences between the stations rather than the annual cycles at individual stations. (With 79 stations the global r must be greater than about 0.22 to be significantly different from 0 at the 95% confidence level, but individual regions have fewer stations and need larger values of r for statistical significance.) In every month the global correlation coefficient differs significantly from zero at the 95% level, and in every month except March and November, when the correlation barely misses, the correlation is significant at the 99% level. The global $r > 0.6$ in June through October, but $r < 0.4$ in November through April (except for January), being particularly low in March and November. Tropical stations are well simulated except for November. We wondered why the model results seemed particularly poor in March and November: does the model not handle STE well or some seasonal transition that occurs then? This is unclear, but later results show that the difference between the high r in July and the low r in March is a few extreme stations as well as the relatively small range of concentrations in March. On the other hand, we note that r is one statistic with a hint of a 6-month seasonal shift between stations with similar latitudes in the northern and southern hemisphere (compare the 30°–60° latitude belts).

The modeled seasonality generally correlates well with observed seasonality at the 79 stations ($r = 0.72$ for Figure 8), but the bias appears because generally $m < o$ in December through February and $m > o$ in March through November.

For the 79 stations in Figure 9*a*, $\bar{m}$ and $\bar{o}$ correlate with

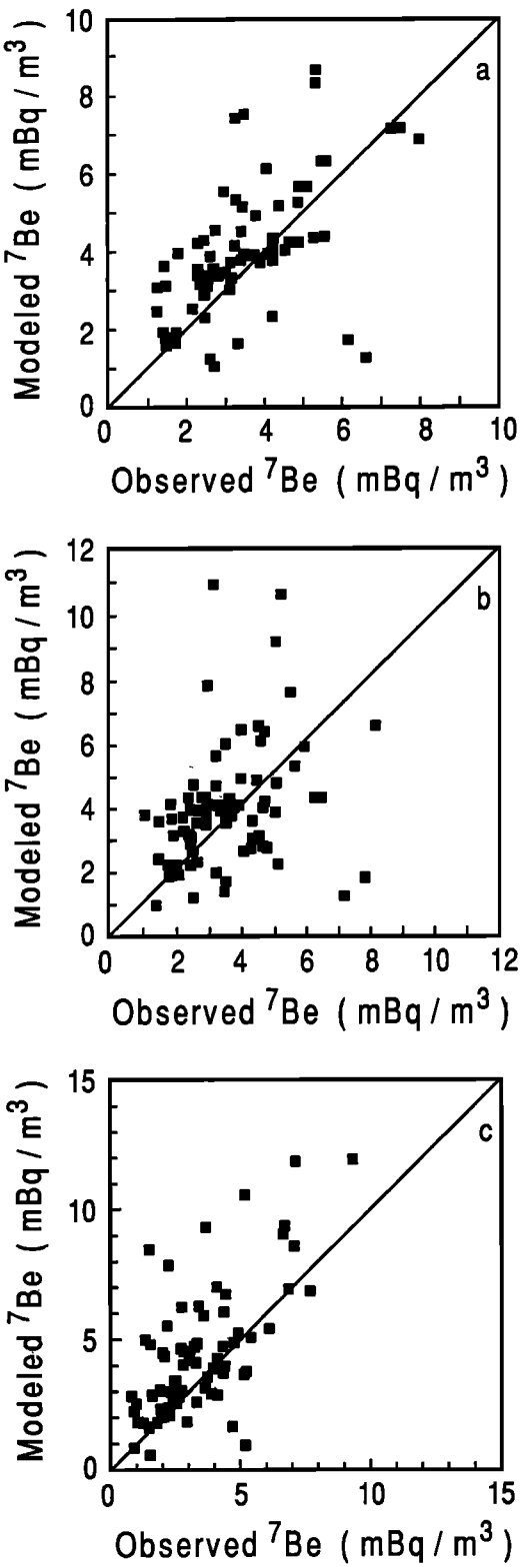

Fig. 9. Modeled versus observed ^{7}Be station concentration for (*a*) the annual average values, (*b*) values during March, and (*c*) July.

r = 0.57. Let us discuss the problem stations. First, to the bottom and lower right of the figure are polar stations, which have $\bar{o} \gg \bar{m}$. The two stations with $\bar{o}$ = 6–7 mBq m^{-3} and $\bar{m}$ = 1–2 mBq m^{-3} are Mawson and Dumont D'Urville in Antarctica; these are affected by katabatic winds, which are not present in the model and lead to severe underprediction there. (*Hogan* [1979] showed that particles at the South Pole Station were carried there by middle tropospheric convergence and subsidence over Antarctica. This circulation would bring down large, middle tropospheric values of ^{7}Be to the Antarctic plateau and, through the katabatic winds, to Mawson and Dumont D'Urville. This circulation is not apparent in the model results.) The four stations that almost line up between ($\bar{o}$ = 2.7, $\bar{m}$ = 1.3) and ($\bar{o}$ = 4.6, $\bar{m}$ = 2.4) are three stations around the periphery of Greenland (Nord, Kap Tobin, and Thule) and South Pole Station. Removing these six polar stations would leave stations in which generally $\bar{m}$ slightly exceeds $\bar{o}$. Second, the four stations in the top center of Figure 9*a*, where $\bar{m} \gg \bar{o}$, are as follows: Chacaltaya, Bolivia; Pico Espejo, Venezuela; Izania, Teneriffe; and Bombay, India (see Table 3). For three of the four stations the observed records are relatively short and of limited climatological significance, and for two of the stations the data are also relatively old: early 1960s for Bombay and early 1970s for Pico. Because of the high elevations of three stations the model simulates relatively high concentrations, but the observed values are much smaller, perhaps because of persistent upslope conditions (bringing up lower concentrations from below) or because of a local, strong precipitation and scavenging that occurs in nature but not in the model. We expect $\bar{m}$ and $\bar{o}$ to increase with elevation in the troposphere, and the decrease in $\bar{o}$ with increasing elevation from La Aguada to Pico Espejo must be of limited statistical significance (involving stations with 21 and 22 months of data) and, if true, must be produced by a local effect (in mountainous terrain) that no global model should be expected to reproduce. Chacaltaya has 174 months of data, so that we cannot dismiss the discrepancy there, but again local effects may be responsible. Restricting ourselves to data collected since 1980 would preferentially eliminate some old questionable data and some problem stations and provide a modest increase in correlation coefficient.

The same problem stations that affected the comparison of annual average concentration also show up as problems during March (Figure 9*b*) but not during July (Figure 9*c*). Figure 9*b* only has r = 0.29, and the low correlation is at least partly caused by Mawson and Dumont D'Urville in the lower right corner of the figure and Pico Espejo and Chacaltaya in the upper left of the figure, although the central cluster in Figure 9*b* seems somewhat more scattered than in Figures 9*a* or 9*c*. In Figure 9*c* these four stations have moved much closer to the central cluster of stations, and the central cluster itself seems tighter, so that r = 0.70.

4.2.2. *Geographical regions.* We have divided our 79 stations into six geographic regions: in each region the comparison of the annual cycle of modeled and observed ^{7}Be surface concentration generally gives a similar level of agreement or similar discrepancies. (There are a few remote island stations that do not fit into these six geographic groups.) In three of the six regions we consider the model simulation, with some reservations perhaps, to be quite good: (1) subtropical (primarily Caribbean) stations; (2) coastal Australia, New Zealand, and surrounding island stations; and (3) middle-latitude, midcontinental stations, where we have the most stations and the most data. The last three groups have some consistent problems: (4) sea level stations under the (positionally fixed) subtropical highs, which usually occur along the west coasts of large continents (the Americas and Africa); (5) Arctic stations; and (6)

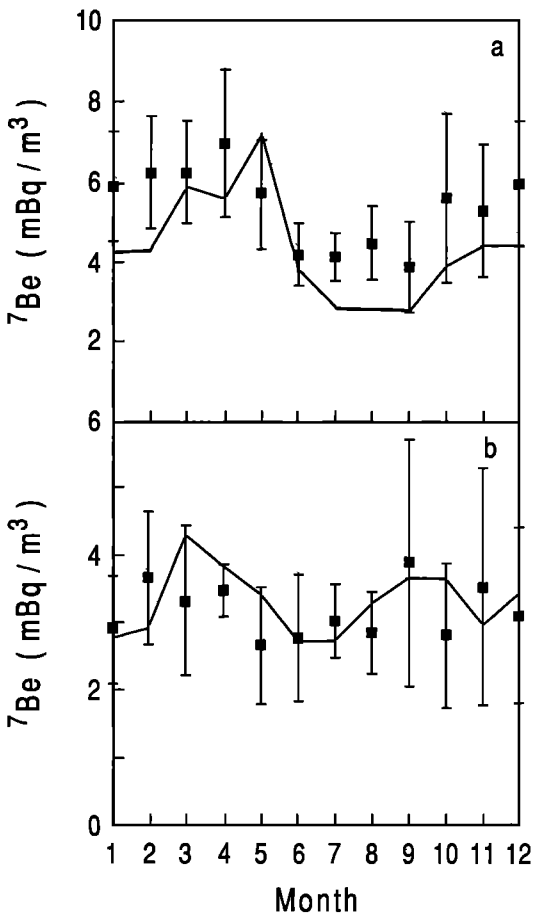

Fig. 10. Monthly average ^{7}Be concentration: solid curve is modeled concentration m, solid squares are observed concentration o, and vertical lines represent $o \pm \sigma_o$. Values at (*a*) Miami, Florida, and (*b*) Cape Grim, Australia.

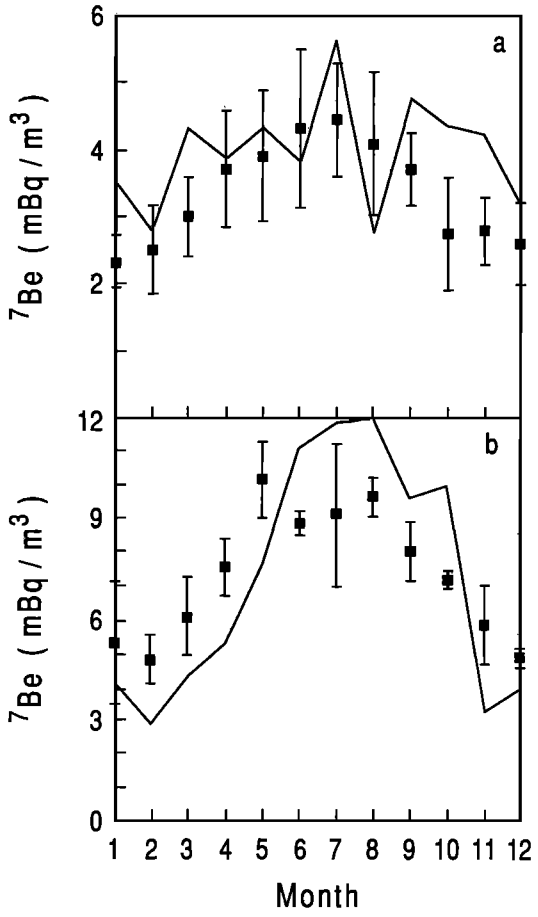

Fig. 11. Monthly average ^{7}Be concentration (see code for Figure 10). Values at (*a*) Fribourg, Switzerland, and (*b*) Salt Lake City, Utah.

Antarctic stations; but remember that regions (5) and (6) represent a small geographic area with few stations, and the errors in region (4) are consistent but not large.

First, the Caribbean region is one of the best simulated regions. *Feely et al.* [1988] showed that there is a strong negative correlation (−0.76 to −0.96) between monthly average precipitation and monthly average surface concentration o at many stations from 14° to 26° latitude in North and South America, which implies that the annual cycle of o is controlled by the annual cycle of wet scavenging. The model simulates the annual cycles well (and those cycles are almost identical) at Miami (Figure 10*a*), Balboa, Merida, La Aguada, and Pico Espejo; only at the last station is $\bar{m}$ not close to $\bar{o}$. Figure 10*a* (Miami, Florida) shows a comparison that typifies the model's performance in this region. During 8 months of the modeled year, m lies within $o \pm \sigma_o$, with σ_o being the standard deviation of the observations for individual Januaries about the long-term average for January and similarly for other months. In January and February, m just barely misses being within σ_o of o, and in July and August m misses because σ_o is abnormally small. At Chacaltaya, Bolivia, the mean concentration and the timing of the seasonal cycle are well simulated, but the modeled amplitude of the seasonal cycle exceeds the observed amplitude ($A_m > A_o$). (We consider Chacaltaya as a transitional station between subtropical and middle-latitude stations).

Second, Figure 10*b* for Cape Grim is typical of the good results found for sea level stations around Australia, New Zealand, and surrounding islands; in every month, m falls within $o \pm \sigma_o$.

Third, the largest amount of data has been taken at middle latitudes over continents, mostly over North America and northwestern Europe. Figures 11*a* and 11*b* show warm season maxima of concentration, whose timing is well simulated by the model, although a single model year has a larger amplitude annual cycle and more month-to-month variability than observations averaged for many years. Here, σ_o is surprisingly small compared to o and to A_o; although m is often outside $o \pm \sigma_o$, the large seasonal variation is generally well represented. Both A_o and A_m grow moving from east to west across North America (not shown); perhaps this increase in annual amplitude is produced by decreasing precipitation and by increasing station elevation, so that higher stations also have larger A_o and A_m. Within a few hundred kilometers of the west coast and as the station elevation approaches sea level, A_o and A_m decrease again, as shown by Tracy, California (Figure 12*a*), which is separated by the coastal mountain range from Richmond, California (Figure 12*b*), which is beside the Pacific Ocean.

Tracy and Richmond are so close that simulated concentrations are essentially identical, whereas o at Richmond has an obvious bite taken out during summer [*Feely et al.*, 1988]. This suggests scavenging by drizzle in the persistent fog and

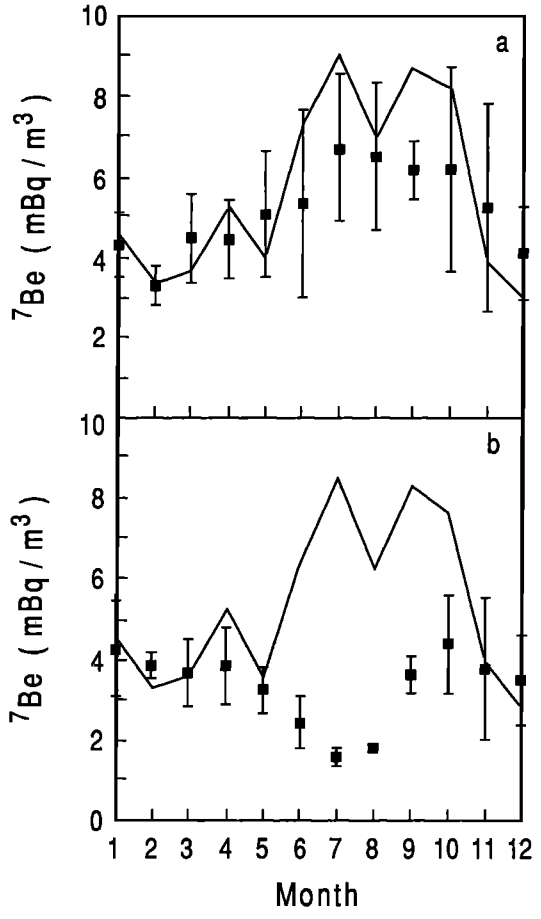

Fig. 12. Monthly average ^{7}Be concentration (see Figure 10). Values at (*a*) Tracy, California, and (*b*) Richmond, California.

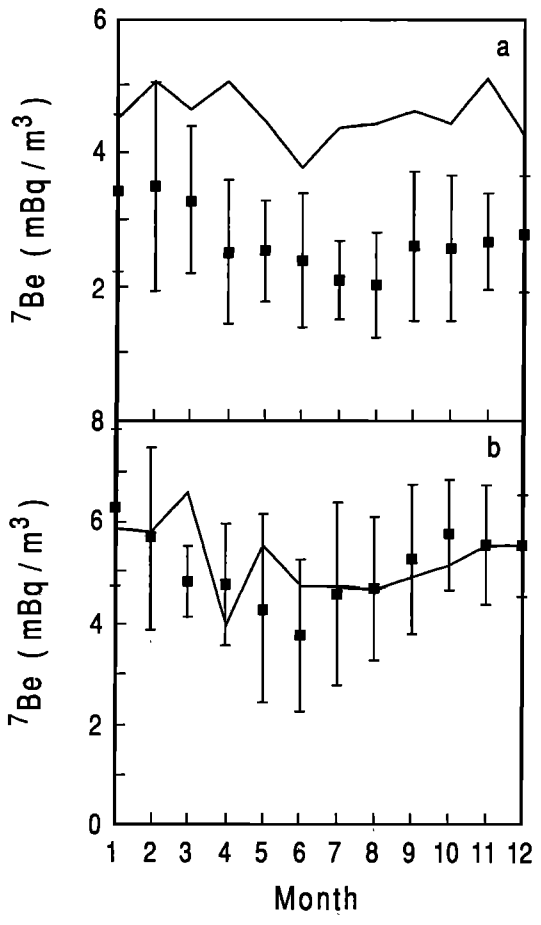

Fig. 13. Monthly average ^{7}Be concentration (see Figure 10). Values at (*a*) Easter Island and (*b*) Santiago, Chile.

stratus found under the subtropical highs during summer. Because we scavenge on the basis of precipitation, there is little scavenging in the model in this region, which we consider our fourth region. Results at Beaverton, Oregon (not shown) give a hint of the same missing scavenging during summer in the model, as do results at the chain of stations along the west coast of South America. This overprediction extends from South America out to Easter Island (Figure 13*a*), where $m > o - \sigma_o$ for 10 of 12 months and just misses being high in every month. On the other hand, above the marine boundary layer in the same region the model simulation can produce good results, as in Santiago, Chile (Figure 13*b*, elevation 520 m).

In contrast to the overprediction at sea level stations under the subtropical highs, there is a general underprediction of concentration at (non-European) sea level stations in the Arctic, our fifth region, and at some stations in Antarctica, our sixth region. Aside from northern Europe the best results found in the Arctic are shown in Figure 14*a* for DYE-3, Greenland (z = 2560 m). The observations, which show a double peak in spring and fall, are a single year of data (J. E. Dibb, private communication, 1990). The simulated annual cycle also has a double peak: in March, 1 month before the observed spring peak; and in September in the middle of the observed fall maximum. At Thule, Greenland (Figure 14*b*), o mimics the observed seasonal pattern of Arctic haze at sea level, a pattern that the model totally misses, although the modeled annual cycle at z = 1–3 km agrees better with the observed cycle at sea level than the modeled cycle at sea level does (compare Figures 14*a* and 14*b*). The lack of agreement in Figure 14*b* is typical of the three stations around the periphery of Greenland.

The sixth group consists of Antarctic stations. It is of course quite interesting to compare three stations that have similar latitudes and elevations but mainly differ in longitude (Chilean Antarctic Station, Mawson, and Dumont d'Urville, see Table 3). At the three stations, $\bar{m}$ is almost identical (1.3–1.7 mBq m^{-3}), but $\bar{o}$ = 1.5 mBq m^{-3} at Antarctic Station, and $\bar{o}$ = 6.2 – 6.7 at the other two. In fact, $\bar{o}$ at Mawson and Dumont d'Urville is exceeded only by $\bar{o}$ at a few stations with $z > 1.5$ km and much lower latitudes, but the role of katabatic winds in the high o at these stations was already discussed. The Antarctic station that is farthest from the pole, also at sea level but not affected in a dominant manner by katabatic winds, is the Chilean Antarctic Station (Figure 14*c*), where the model does quite well in representing $\bar{o}$ and the lack of an annual cycle. We do not know why the observed annual cycle at the South Pole Station resembles that at sea level in the Arctic, without a 6-month shift, but we believe that the observed cycle in polar regions does not result from an annual cycle in the source term (Figure 14*d*).

5. Conclusions

We suggest that the simulation of ^{7}Be and ^{210}Pb might establish the standards for how well a model can represent

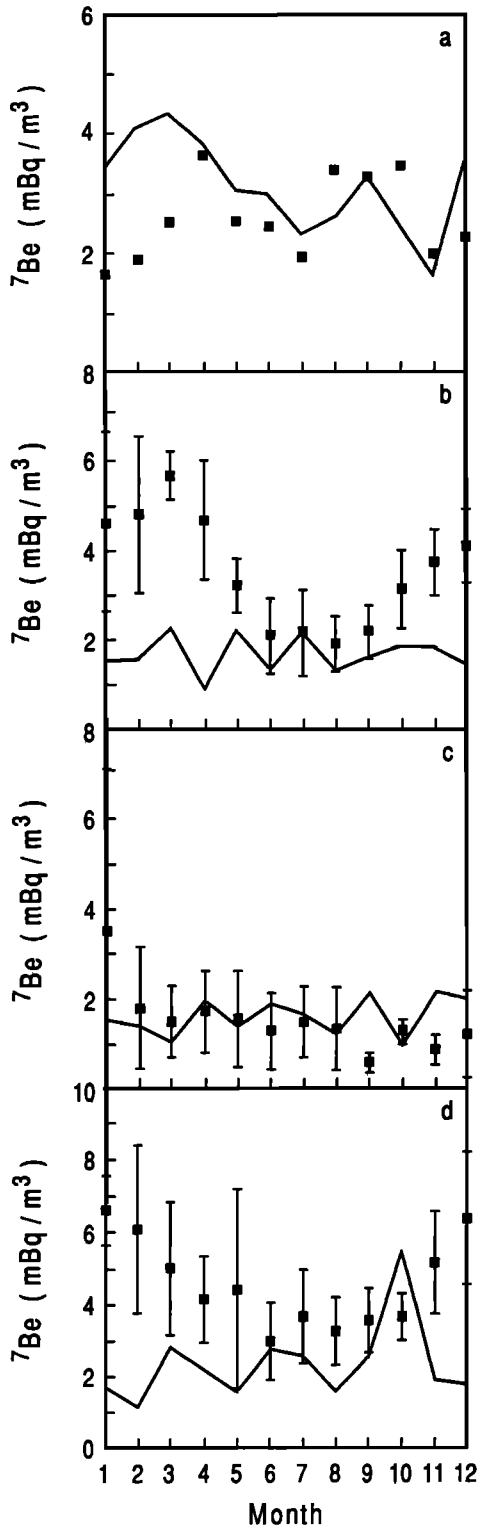

Fig. 14. Monthly average ^{7}Be concentration (see Figure 10). A single year of monthly average ^{7}Be concentration at DYE-3, Greenland: solid curve is modeled and solid squares are observations of J. E. Dibb (private communication, 1990). (*b*) Conditions at Thule, Greenland (see Figure 10 for code). (*c*) Chilean Antarctic Station. (*d*) South Pole Station.

the concentration and deposition of an aerosol species because these two species have large amounts of climatologically significant data in conjunction with relatively well-known sources and "chemistry." On first appearance we seemed to find generally good results modeling ^{7}Be, but we must be careful about our standard of comparison. Monthly average surface concentration of ^{7}Be varies from about 1–10 mBq m^{-3}, with most observations between 2 and 8 mBq m^{-3}, so that a model that always predicted a constant surface value of 4 mBq m^{-3} would almost always be within a factor of 2 of the observed surface concentration. The point is therefore that the model-simulated concentration m must certainly be closer than a factor of 2 to the observed concentration o to be considered a good simulation. Not only do we want to get the annual average concentration correctly, but we would like to get the monthly average values correctly, in particular, the timing and amplitude of the seasonal cycle. Even by these high standards we believe that we find remarkably good agreement between the simulated and observed climatological concentrations at most of the 79 surface stations.

Most of the stations with surface concentration observations fell into six regional groups: (1) Caribbean stations; (2) middle-latitude, midcontinental stations; (3) coastal areas in or near Australia; (4) coastal regions under the positionally fixed subtropical highs; (5) Arctic stations; and (6) Antarctic stations. The modeled concentration compared well with observations for the first three groups, which contain the bulk of the data and describe the majority of the geographic area with data, although the simulated annual cycle was often too large over middle-latitude continents. The simulated concentrations were often too large under the subtropical highs and too small in polar regions. When there were significant observed annual cycles of monthly average concentration, the model tended to place the maxima and minima in the correct seasons except in polar regions.

Several of the problems found in comparing simulations with observations are consistent with known problems in the meteorological climatology of ECHAM2 (E. Roeckner, private communication, 1990). First, because of the spectral advection scheme the model produces too much precipitation in polar regions, which is consistent with the low simulated concentrations there, although the discrepancy in ^{7}Be concentration there may be produced by poor transport and not by excessive wet scavenging. Second, the high simulated concentrations over middle-latitude continents during summer are consistent with the anomalously low precipitation simulated by the model there.

The usefulness of ^{7}Be as a test of scavenging depends on the fraction of stations at which the observed ^{7}Be concentration depends on local effects, such as katabatic flows, mountain-valley winds, and local fog and stratus, because the large grid cells of the climatological, global model could not be expected to represent such small-scale effects. We have pointed out that only a minority of the stations seem to be contaminated by such effects. (The stratus often found under the subtropical high pressure system must be parameterized in ECHAM2, so that the scavenging effect of such stratus needs a special parameterization that is independent of the precipitation rate.)

We used a simple scavenging scheme that used only the rate of condensation in a grid cell in each model time step Δt = 40 min to determine the cloud coverage in the cell and the fraction of tracer in the cloudy portion of the cell that was scavenged in Δt, and then remixed the clear and cloudy portion of the cell after each step. Essentially the same scavenging scheme has been used for very soluble species by

GC86, for background tropospheric aeosols here, for continental PBL aerosols by *Feichter et al.* [this issue], and for soot by *Bakan et al.* [1991]. Changes in the constants were necessary to represent the solubility of different aerosols and solubility and reactivity of different gaseous species. This paper and *Feichter et al.* [this issue] showed how well such a simple scheme in representing the scavenging of aerosol species when the scheme did not retain, from time step to time step, information on the tracer mixing ratio in the clear and cloudy portions of the grid cells. In general, the concentration and deposition of the two species could be matched to within 20%; however, simulating deposition and concentration in polar regions is inadequate with this transport model and scavenging scheme. Perhaps better resolution would also provide better downward transport or diffusion to the surface in the Arctic and hence a better simulation of the seasonal cycle at sea level in the Arctic. A better scavenging parameterization might also improve the agreement that we found here.

Also, future work should increase the size of the data set used for comparison, and make more detailed comparisons with the observed deposition and vertical profile of concentration. The highest priority should be to collect and publish more deposition data. In particular, we need multiple years of deposition data to have an idea of the interannual variability. We also need deposition data in additional geographical and latitudinal regions (places other than North America and Europe), especially in polar regions and near the ITCZ in order to see whether there should be a deposition maximum or minimum near the equator. The next priority would be to collect additional vertical profiles and time series data at different heights in the troposphere, again, particularly in polar regions. The collection, compilation, and publishing of additional data on surface concentration should also be encouraged.

Acknowledgments. We wish to thank Bill Graustein for pointing out what an interesting pair ^{7}Be and ^{210}Pb would make as well as providing some data, Daniel Jacob for telling us about the EML data, and Richard Larsen for promptly providing the EML data. In addition, many other people have kindly provided useful references, discussions, and data: Asker Aarkrog, Richard Arimoto, A. Bayer, Jack Dibb, Vince Dutkiewicz, Dieter Ehhalt, Colin Johnson, H. Keller, W. Kolb, K. M. Matthews, C. Rangarajan, Daniel Robeau, K. Roehrs, Wolfgang Seiler, Rudolf Sládkovič, and Mitsuo Uematsu. We would particularly like to acknowledge useful discussions with Chip Levy, Jerry Mahlman, Heather Marshall, and Devendra Lal, and we apologize to anyone we may have forgotten to thank.

REFERENCES

Aegerter, S., N. Bhandari, Rama, and A. S. Tamhane, ^{7}Be and ^{32}P in ground level air, *Tellus*, *18*, 212–215, 1966.

Arnold, J. R., and H. A. Al-Salih, Beryllium-77 produced by cosmic rays, *Science*, *121*, 451–453, 1955.

Bakan, S., et al., Climate response to smoke from burning oil wells in Kuwait, *Nature*, *351*, 367–371, 1991.

Barnett, T. P., L. Duemenil, U. Schlese, E. Roeckner, and M. Latif, The effect of Eurasian snow cover on regional and global climate, *J. Atmos. Sci.*, *46*, 661–685, 1989.

Bhandari, N., Transport of air in the stratosphere as revealed by radioactive tracers, *J. Geophys. Res.*, *75*, 2927–2930, 1970*a*.

Bhandari, N., Vertical structure of the troposphere as revealed by radioactive tracer studies, *J. Geophys. Res.*, *75*, 2974–2980, 1970*b*.

Bhandari, N., D. Lal, and Rama, Stratospheric circulation studies based on natural and artificial radioactive tracer elements, *Tellus*, *18*, 391–405, 1966.

Bleichrodt, J. F., Mean tropospheric residence time of cosmic-ray-produced Beryllium 7 at north temperate latitudes, *J. Geophys. Res.*, *83*, 3058–3062, 1978.

Boer, G. J., N. A. McFarlane, R. Laprise, J. D. Henderson, and J. P. Blanchet, The Canadian Climate Centre spectral atmospheric general circulation model, *Atmos. Ocean*, *22*, 397–429, 1984.

Brown, L., G. J. Stensland, J. Klein, and R. Middleton, Atmospheric deposition of ^{7}Be and ^{10}Be, *Geochim. Cosmochim. Acta.*, *53*, 135–142, 1989.

Cess, R. D., et al., Interpretation of cloud-climate feedback as produced by 14 atmospheric general circulation models, *Science*, *245*, 513–516, 1989.

Commissariat à l'Energie Atomique, Surveillance de la Radioactivité de l'Environnement des Installations du Groupe CEA, edited by Laboratoire d'Etudes Sanitaires, report for 3rd trimester, 1987, Fontenay-aux-Roses, France, 1987*a*.

Commissariat à l'Energie Atomique, Surveillance de la Radioactivité de l'Environnement des Installations du Groupe CEA, edited by Laboratoire d'Etudes Sanitaires, report for 4th trimester, 1987, Fontenay-aux-Roses, France, 1987*b*.

Commissariat à l'Energie Atomique, Surveillance de la Radioactivité de l'Environnement des Installations du Groupe CEA, edited by Laboratoire d'Etudes Sanitaires, report for 1st trimester, 1988, Fontenay-aux-Roses, France, 1988*a*.

Commissariat à l'Energie Atomique, Surveillance de la Radioactivité de l'Environnement des Installations du Groupe CEA, edited by Laboratoire d'Etudes Sanitaires, report for 2nd trimester, 1988, Fontenay-aux-Roses, France, 1988*b*.

Commissariat à l'Energie Atomique, Surveillance de la Radioactivité de l'Environnement des Installations du Groupe CEA, edited by Laboratoire d'Etudes Sanitaires, report for 3rd trimester, 1988, Fontenay-aux-Roses, France, 1988*c*.

Commissariat à l'Energie Atomique, Surveillance de la Radioactivité de l'Environnement des Installations du Groupe CEA, edited by Laboratoire d'Etudes Sanitaires, report for 4th trimester, 1988, Fontenay-aux-Roses, France, 1988*d*.

Commissariat à l'Energie Atomique, Surveillance de la Radioactivité de l'Environnement des Installations du Groupe CEA, edited by Laboratoire d'Etudes Sanitaires, report for 1st trimester, 1989, Fontenay-aux-Roses, France, 1989*a*.

Commissariat à l'Energie Atomique, Surveillance de la Radioactivité de l'Environnement des Installations du Groupe CEA, edited by Laboratoire d'Etudes Sanitaires, report for 2nd trimester, 1989, Fontenay-aux-Roses, France, 1989*b*.

Commissariat à l'Energie Atomique, Synthèse Mensuelle des Mesures de Radioactivité Effectuées dans l'Environnement des Sites du Groupe CEA, edited by Département de Protection Sanitaire, *Rapp. DPS 90/001/2*, Fontenay-aux-Roses, France, 1990*a*.

Commissariat à l'Energie Atomique, Synthèse Mensuelle des Mesures de Radioactivité Effectuées dans l'Environnement des Sites du Groupe CEA, edited by Département de Protection Sanitaire, *Rapp. DPS 90/001/3*, Fontenay-aux-Roses, France, 1990*b*.

Commissariat à l'Energie Atomique, Synthèse Mensuelle des Mesures de Radioactivité Effectuées dans l'Environnement des Sites du Groupe CEA, edited by Département de Protection Sanitaire, *Rapp. DPS 90/001/4*, Fontenay-aux-Roses, France, 1990*c*.

Commissariat à l'Energie Atomique, Synthèse Mensuelle des Mesures de Radioactivité Effectuées dans l'Environnement des Sites du Groupe CEA, edited by Département de Protection Sanitaire, *Rapp. DPS 90/001/5*, Fontenay-aux-Roses, France, 1990*d*.

Crecelius, E. A., Prediction of marine atmospheric deposition rates using total ^{7}Be deposition velocities, *Atmos. Environ.*, *15*, 579–582, 1981.

Cruikshank, A. J., G. Cowper, and W. E. Grummitt, Production of ^{7}Be in the atmosphere, *Can. J. Chem.*, *34*, 214–219, 1956.

Cubasch, U., R. Sausen, J. Oberhuber, F. Lunkeit, and M. Boettinger, Simulation of the greenhouse effect with coupled ocean-atmosphere models, *Cray Channels*, *12*, 6–9, 1990.

Dibb, J. E., Atmospheric deposition of Beryllium 7 in the Chesapeake Bay region, *J. Geophys. Res.*, *94*, 2261–2265, 1989.

Drevinsky, P. J., J. T. Wasson, E. C. Couble, and N. A. Dimond, ^{7}Be, ^{32}P, ^{33}P, and ^{32}S: Stratospheric concentrations and artificial production, *J. Geophys. Res.*, *69*, 1457–1467, 1964.

Duemenil, L., and U. Schlese, Description of the general circulation model, in *Climate Simulations With the ECMWF T21-Model in Hamburg*, edited by G. Fischer, *Rep. 1*, Meteorol. Inst. of the Univ. of Hamburg, Germany, 1987.

Dutkiewicz, V. A., Tracer transport applied to atmospheric transport studies, in *Proceedings of the International Nathiagali Summer College on Physics and Comtemporary Needs*, vol. 7, Islamabad, Pakistan, July 31–August 19, 1982, edited by M. N. Qazi, pp. 62–94, World Scientific Publishing Company, Singapore, 1985.

Dutkiewicz, V. A., and L. Husain, Determination of stratospheric ozone at ground level using ^{7}Be/ozone ratios, *Geophys. Res. Lett.*, *6*, 171–174, 1979.

Dutkiewicz, V. A., and L. Husain, Stratospheric and tropospheric components of ^{7}Be in surface air, *J. Geophys. Res.*, *90*, 5783–5788, 1985.

Feely, H. W., R. J. Larsen, and C. G. Sanderson, Annual report of the surface air sampling program, July 1988, *Rep. EML-497*, Environ. Meas. Lab., U.S. Dept. of Energ., New York, 1988. (Available from NTIS, Natl. Tech. Inf. Serv., Springfield, VA.)

Feichter, J., and P. J. Crutzen, Parameterization of vertical tracer transport due to deep cumulus convection in a global transport model and its evaluation with ^{222}Radon measurements, *Tellus*, *42(B)*, 100–117, 1990.

Feichter, J., E. Roeckner, and M. Windelband, Tracer transport in the Hamburg climate model, in *Proceedings of 18th International Technical Meeting on Air Pollution Modelling and its Application*, edited by H. van Dop, pp. 497–506, Plenum, New York, 1991.

Feichter, J., R. A. Brost, and M. Heimann, Three-dimensional modeling of the concentration and deposition of ^{210}Pb aerosols, *J. Geophys. Res.*, this issue.

Friedlander, M. W., Cosmic rays: *Tracking Particles From Outer space*, 160 pp., Harvard University Press, Cambridge, Mass., 1989.

Giorgi, F., and W. L. Chameides, Rainout lifetimes of highly soluble aerosols and gases as inferred from simulations with a general circulation model, *J. Geophys. Res.*, *91*, 14,367–14,376, 1986.

Gopalakrishnan, S., C. Rangarajan, L. U. Joshi, D. K. Kapoor, and C. D. Eapen, Measurements of airborne and surface fallout radioactivity in India, *BARC679*, Govt. of India, At. Energ. Comm., Bhabha At. Res. Cent., Bombay, India, 1973.

Hales, J. M., The mathematical characterization of precipitation scavenging and precipitation chemistry, in *The Handbook of Environmental Chemistry*, vol. 4, part A, edited by O. Hutzinger, pp. 149–217, Springer-Verlag, New York, 1986.

Harvey, M. J., and K. M. Matthews, ^{7}Be deposition in a high-rainfall area of New Zealand, *J. Atmos. Chem.*, *8*, 299–306, 1989.

Heimann, M., and J. Feichter, A comparison of three-dimensional atmospheric transport models by means of simulations of Radon-222, *Rep. 8*, Meteorol. Inst., Univ. Hamburg, Germany, 1990.

Heimann, M., and C. D. Keeling, A three-dimensional model of atmospheric CO_2 transport based on observed winds, 2, Model description and simulated tracer experiments, in *Aspects of Climate Variability in the Pacific and the Western Americas*, edited by D. H. Peterson, AGU, Washington, D. C., 1989.

Hillas, A. M., *Cosmic Rays*, 297 pp., Pergamon, New York, 1972.

Hogan, A. W., Meteorological transport of particulate material to the South Polar Plateau, *J. Appl. Meteorol.*, *18*, 741–749, 1979.

Hoetzl, H., G. Rosner, and R. Winkler, Correlation of ^{7}Be concentrations in surface air and precipitation with the solar cycle, *Naturwissenschaften*, *78*, 215–217, 1991.

Joussaume, S., Three-dimensional simulations of the atmospheric cycle of desert dust particles using a general circulation model, *J. Geophys. Res.*, *95*, 1909–1941, 1990.

Junge, C. E., *Air Chemistry and Radioactivity*, 382 pp., Academic, San Diego, Calif., 1963.

Junge, C. E., Processes responsible for tracer content in precipitation, in Proceedings of the Grenoble Symposium on Isotopes and Impurities in Snow and Ice, August–September 1975, *IAHS-AISH Publ. 118*, 63–77, 1977.

Junge, C. E., and P. E. Gustafson, On the distribution of sea salt over the United Sates and its removal by precipitation, *Tellus*, *9*, 164–173, 1957.

Kolb, W., Jahreszeitliche Schwankungen der ^{7}Be-, ^{54}Mn- und Splatprodukt-Konzentrationen der bodennahen Luft, *Tellus*, *22*, 443–450, 1970.

Kolb, W., Einfluss chinesischer Kernwafftenversuche auf die Radionuklid-Konzentration in der bodennahen Luft, *Ber. Ra 1-71*, *Phys.-Tech. Bundesanst.*, Laboratorium für Strahlenschutz, Braunschweig, Germany, 1971.

Kolb, W., Radionuclide concentrations in ground level air from 1971 to 1973 in Brunswick and Tromso, *Ber. Ra-4*, *Phys.-Tech. Bundesanst.*, Laboratorium für Strahlenschutz, Braunschweig, Germany, 1974.

Kolb, W., Radionuclide concentrations in ground level air from 1974 to 1977 in North Germany and North Norway, *PTB Ra-9*, *Phys.-Tech. Bundesanst.*, Laboratorium für Strahlenschutz, Braunschweig, Germany, 1978.

Kolb, W., Radionuclide concentrations in ground level air from 1978 to 1979 in North Germany and North Norway, *PTB Ra-11*, *Phys.-Tech. Bundesanst.*, Laboratorium für Strahlenschutz, Braunschweig, Germany, 1980.

Kolb, W., Radionuclide concentrations in ground level air from 1980 to 1983 in North Germany and North Norway, *PTB Ra-15*, *Phys.-Tech. Bundesanst.*, Laboratorium für Strahlenschutz, Braunschweig, Germany, 1984.

Kolb, W., Radionuclide concentrations in ground level air from 1984 to 1986 in North Germany and North Norway, *PTB Ra-18*, *Phys.-Tech. Bundesanst.*, Laboratorium für Strahlenschutz, Braunschweig, Germany, 1986.

Kolb, W., Radionuclide concentrations in ground level air from 1986 to 1987 in North Germany and North Norway, *PTB Ra-21*, *Phys.-Tech. Bundesanst.*, Laboratorium für Strahlenschutz, Braunschweig, Germany, 1988.

Kolb, W., Radionuclide concentrations in ground level air from 1988 to 1989 in North Germany and North Norway, *PTB Ra-25*, *Phys.-Tech. Bundesanst.*, Laboratorium für Strahlenschutz, Braunschweig, Germany, 1990.

Kuo, H. L., Further studies of the parameterization of the influence of cumulus convection on large scale flow, *J. Atmos. Sci.*, *31*, 1232–1240, 1974.

Lal, D., On the investigations of geophysical processes using cosmic ray produced radioactivity, in *Earth Science and Meteoritics*, compiled by J. Geiss and E. D. Goldberg, 312 pp., North-Holland, New York, 1963.

Lal, D., and B. Peters, Cosmic ray produced isotopes and their applications to problems in geophysics, in *Progress in Cosmic Ray and Elementary Particle Physics*, vol. 6, pp. 3–74, North-Holland, New York, 1962.

Lal, D., and B. Peters, Cosmic ray produced radioactivity on the earth, *Handb. Phys.*, *46*, 551–612, 1967.

Lal, D., Rama, and P. K. Zutshi, Radioisotopes ^{32}P, ^{7}Be, and ^{33}S in the atmosphere, *J. Geophys. Res.*, *65*, 669–674, 1960.

Lambert, G., B. Ardouin, and J. Sanak, Atmospheric transport of trace elements toward Antarctica, *Tellus*, *42(B)*, 76–82, 1990.

Larsen, R. J., and C. G. Sanderson, Annual report of the surface air sampling program, February 1990, *Rep. EML-524*, Environ. Meas. Lab., U.S. Dep. of Energy, New York, 1990. (Available from NTIS, Natl. Tech. Inf. Serv., Springfield, Va.)

Latif, M., J. Biercamp, H. v. Storch, M. J. McPhaden, and E. Kirk, Simulation of ENSO related surface wind anomalies with an atmospheric GCM forced by observed SST, *J. Clim.*, *3*, 509–521, 1990.

Laursen, L., and E. Eliasen, Sensitivity of a spectral general circulation model to changes in the parameterizations of the mechanical processes, *Rep. 12*, *WMO/TD-273*, 207–214, 1988.

Levy, H., II, and W. J. Moxim, The fate of US and Canadian combustion emissions, *Nature*, *328*, 414–416, 1987.

Levy H., II, and W. J. Moxim, Simulated global distribution and deposition of reactive nitrogen emitted by fossil fuel combustion, *Tellus*, 41(B), 256–271, 1989.

Levy, H., II, J. D. Mahlman, and W. J. Moxim, A stratospheric source of reactive nitrogen in the unpolluted troposphere, *Geophys. Res. Lett.*, *7*, 441–444, 1980.

Luder, R., ^{10}Be and ^{7}Be in Niederschlagen und Luftfiltern, diploma thesis, Phys. Inst. der Univ. Bern, Bern, Switzerland, 1985.

Mahlman, J. D., and W. J. Moxim, Tracer simulation using a global general circulation model: Results from a mid-latitude instantaneous source experiment, *J. Atmos. Sci.*, *35*, 1340–1378, 1978.

Marenco, A., and J. Fontan, Etude des Variations des ^{7}Be, ^{32}P, ^{90}Sr, ^{210}Pb, et ^{210}Po dans la troposphère, *Tellus*, *26*, 386–401, 1974.

Mason, B. J., *The Physics of Clouds*, 481 pp., Oxford University Press, New York, 1957.

Matsushita, S., and H. Campbell, *Physics of Geomagnetic Phenomena*, vol. 2, 1329 pp., Academic, San Diego, Calif., 1967.

Matthews, K. M., Environmental radioactivity annual report 1988, *NRL-F/68*, Dep. of Health, Natl. Radiat. Lab., Christchurch, N. Z., 1989.

Matthews, K. M., Environmental radioactivity annual report 1989, *NRL-F/69*, Dep. of Health, Natl. Radiat. Lab., Christchurch, N. Z., 1990.

O'Brien, K., Secular variations in the production of cosmogenic isotopes in the Earth's atmosphere, *J. Geophys. Res.*, *84*, 423–431, 1979.

Paakkola, O., et al., Studies in environmental radioactivity in Finland 1984–1985, annual report, *STUK Rep. A54*, Surv. Dep. of the Finn. Cent. for Radiat. and Nucl. Safety (STUK), Helsinki, Finland, 1987.

Parker, R. P., Beryllium-7 and fission products in surface air, *Nature*, *193*, 967–968, 1962.

Peirson, D. H., Beryllium-7 in air and rain, *J. Geophys. Res.*, *68*, 3831–3832, 1963.

Penner, J. E., C. S. Atherton, J. Dignon, S. J. Ghan, and J. J. Walton, Tropospheric nitrogen: A three-dimensional study of sources, distributions, and deposition. *J. Geophys. Res.*, *96(D1)*, 959–990, 1991.

Pruppacher, H. R., and J. D. Klett, *Microphysics of Clouds and Precipitation*, 714 pp., D. Reidel, Norwell, Mass., 1978.

Raisbeck, G. M., F. Yiou, M. Fruneau, J. M. Loisseaux, M. Lieuvin, and I. C. Ravel, Cosmogenic ^{10}Be/^{7}Be as a probe of atmospheric transport processes, *Geophys. Res. Lett.*, *8*, 1015–1018, 1981.

Rangarajan, C., and C. D. Eapen, The use of natural radioactive tracers in a study of atmospheric residence times, *Tellus*, *42*(B), 142–147, 1990.

Rangarajan, C., and S. Gopalakrishnan, Seasonal variation of Beryllium-7 relative to Caesium-137 in surface air at tropical and sub-tropical latitudes, *Tellus*, *22*, 115–121, 1970.

Reiter, R., and K. Munzert, Cosmogenic radionuclides at a mountain station under fallout background conditions with consideration of the stratospheric residence time, *Arch. Meteorol. Geophys. Bioklimatol. Ser. B.*, *32*, 187–197, 1983.

Reiter, R., R. Sládkovič, K. Poetzl, W. Carnuth, and H.-J. Kanter, Studies on the influx of stratospheric air into the lower troposphere using cosmic-ray-produced radionuclides and fallout, *Arch. Meterol. Geophys. Bioklimatol., Ser. A*, *20*, 211–246, 1971.

Reiter, E. R., W. Carnuth, H.-J. Kanter, K. Poetzl, R. Reiter, and R. Sládkovič, Measurements of stratospheric residence times, *Arch. Meterol. Geophys. Bioklimatol, Ser. A.*, *24*, 41–51, 1975.

Reiter, R., K. Munzert, H.-J. Kanter, and K. Poetzl, Cosmogenic radionuclides and ozone at a mountain station at 3.0 km a.s.l., *Arch. Meterol. Geophys. Bioklimatol, Ser. B*, *32*, 131–160, 1983.

Rockel, B., B. Zhao, and E. Raschke, A flexible radiative transfer routine for GCM's: Infrared part, in *Research Activities in Atmospheric and Oceanic Modelling*, edited by G. J. Boer, CAS/JSC Working Group on Numerical Experimentation, *Rep. 9*, *WMO/TD-141*, 4.62–4.65, 1986.

Roeckner, E., and U. Schlese, *Proceedings of the ECMWF Workshop on Cloud Cover Parameterization in Numerical Models*, pp. 87–108, Europ. Cent. For Medium-Range Weather Forecasts, Reading, U. K., 1985.

Roeckner, E., L. Duemenil, E. Kirk, F. Lunkeit, M. Ponater, B. Rockel, R. Sausen, and U. Schlese, The Hamburg version of the ECMWF model (ECHAM), in *Research Activities in Atmospheric and Oceanic Modeling*, CAS/JSC Working Group on Numerical Experimentation, *WMO/TD-332*, *Rep. 13*, 7.1–7.4, 1989*a*.

Roeckner, E., U. Schlese, and B. Rockel, The impact of cloud and radiation parameterization changes in January and July simulations with the ECMWF T21 model, in *Climate Simulations With the ECMWF T21-Model in Hamburg*, edited by G. Fischer, Meterol. Inst., Univ. of Hamburg, *Rep.* 7, Germany, 1989*b*.

Roedel, W., Cosmic-ray-produced Sodium 24 and other nuclides in the lower atmosphere, *J. Geophys. Res.*, *75*, 3033–3038, 1970.

Schumann, G., and M. Stoeppler, Beryllium-7 in the atmosphere, *J. Geophys. Res.*, *68*, 3827–3830, 1963.

Shapiro, M. H., and J. L. Forbes-Resha, Mean residence time of ^{7}Be-bearing aerosols in the troposphere, *J. Geophys. Res.*, *81*, 2647–2649, 1976.

Sundquist, H., E. Berge, and J. E. Kristjansson, Condensation and cloud parameterization studies with a mesoscale numerical weather prediction model, *Mon. Weather Rev.*, *117*, 1641–1657, 1989.

Todd, J. F., and G. T. F. Wong, Atmospheric depositional characteristics of Beryllium 7 and Lead 210 along the southeastern Virginia coast, *J. Geophys. Res.*, *94*, 11,106–11,116, 1989.

Toepfer, K., Umweltpolitik: Umweltradioaktivität und Strahlenbelastung Jahresbericht 1986, Der Bundesminister für Umwelt, Naturschutz und Reaktorsicherheit, Bonner Univ. Buchdruckerei, Bonn, 1986.

Turekian, K. K., Y. Nozaki, and L. K. Benninger, Geochemistry of atmospheric radon and radon products, *Annu. Rev. Earth Planet. Sci.*, *5*, *227–255*, *1977*.

Turekian, K. K., L. K. Benninger, E. P. Dion, ^{7}Be and ^{210}Pb total deposition fluxes at New Haven, Connecticut and at Bermuda, *J. Geophys. Res.*, *88*, 5411–5414, 1983.

Viezee, W., and H. B. Singh, The distribution of Beryllium-7 in the troposphere: Implications on stratospheric/tropospheric air exchange, *Geophys. Res. Lett.*, *7*, 805–808, 1980.

Windelband, M., Simulation of the interhemispheric transport of freon11 with an atmospheric circulation model (in German), diploma thesis, Meterol. Inst. Univ. Hamburg, Germany, 1990.

Wolff, G. T., M. A. Ferman, and P. R. Monson, The distribution of beryllium-7 within high-pressure systems in the eastern United States, *Geophys. Res. Lett.*, *6*, 637–639, 1979.

Young, J. A., and W. B. Silker, Aerosol deposition velocities on the Pacific and Atlantic Oceans calculated from ^{7}Be measurements, *Earth Planet. Sci. Lett.*, *50*, 92–104, 1980.

Young, J. A., N. A. Wogman, C. W. Thomas, and R. W. Perkins, Short lived cosmic ray-produced radionuclides as tracers of atmospheric processes, in *Radionuclides in the Environment*, edited by E. C. Frieling, pp. 506–521, American Chemical Society, Washington, D. C., 1970.

Zimmerman, P. H., MOGUNTIA: A handy global tracer model, in *Proceedings of the Sixteenth NATO/CCMS International Technical Meeting on Air Pollution Modeling and Its Application*, edited by H. V. Dop, pp. 593–608, Plenum, New York, 1988.

Zimmerman, P. H., J. Feichter, and P. J. Crutzen, A global three-dimensional source-receptor model investigation using ^{85}Kr, *Atmos. Environ.*, *23*, 25–35, 1989.

R. A. Brost, Max-Planck-Institut für Chemie, Otto Hahn Institut, Postfach 3060, 23 Saarstrasse, W-6500 Mainz, Germany.

J. Feichter, Meteorological Institute, University of Hamburg, Bundesstrasse 55, W-2000, Hamburg 13, Germany.

M. Heimann, Max-Planck Institut für Meterologie, Bandesstrasse 55, W-2000, Hamburg 13, Germany.

(Received March 14, 1991;
revised August 26, 1991;
accepted August 26, 1991.)